ระบบของไหลจุลภาคแบบพกพา สำหรับตรวจวัดปริมาณแคลเซียมด้วยหลักการ Arsenazo III

นางสาวยุวดี บุญญสิทธิ์

วิทยานิพนธ์นี้เป็นส่วนหนึ่งของการศึกษาตามหลักสูตรปริญญาวิทยาศาสตรมหาบัณฑิต
สาขาวิชาชีวเคมีคลินิกและอณูทางการแพทย์ ภาควิชาเคมีคลินิก
คณะสหเวชศาสตร์ จุฬาลงกรณ์มหาวิทยาลัย
ปีการศึกษา 2553

Portable microfluidic system for determination of calcium based on Arsenazo III method

Miss Yuwadee Boonyasit

A Thesis Submitted in Partial Fulfillment of the Requirements for the

Degree of Master of Science Program in Clinical Biochemistry and Molecular Medicine

Department of Clinical Chemistry

Faculty of Allied health Sciences

Chulalongkorn University

Academic Year 2010

Thesis Title	Portable microfluidic system for determination of calcium based on Arsenazo III method
By	Miss Yuwadee Boonyasit
Field of Study	Clinical Biochemistry and Molecular Medicine
Thesis Advisor	Assistant Professor Wanida Laiwattanapaisal, Ph.D.
Thesis Co-advisor	Adisorn Tuantranont, Ph.D.

Accepted by the Faculty of Allied Health Sciences, Chulalongkorn University in Partial Fulfillment of the Requirements for the Master's Degree

…….. Dean of the Faculty of Allied Health Sciences
(Assistant Professor Vanida Nopponpunth, Ph.D.)

THESIS COMMITTEE

…….. Chairman
(Associate Professor Rachana Santiyanont, Ph.D.)

…….. Thesis Advisor
(Assistant Professor Wanida Laiwattanapaisal, Ph.D.)

…….. Thesis Co-advisor
(Adisorn Tuantranont, Ph.D.)

…….. Examiner
(Associate Professor Mana Sriyudthsak, Ph.D.)

…….. External Examiner
(Wijitar Dungchai, Ph.D.)

ยุวดี บุญญสิทธิ์ : ระบบของไหลจุลภาคแบบพกพา สำหรับตรวจวัดปริมาณแคลเซียมด้วยหลักการ Arsenazo III (PORTABLE MICROFLUIDIC SYSTEM FOR DETERMINATION OF CALCIUM BASED ON ARSENAZO III METHOD)
อ. ที่ปรึกษาวิทยานิพนธ์หลัก: ผศ.ดร. วนิดา หลายวัฒนไพศาล, อ. ที่ปรึกษาวิทยานิพนธ์ร่วม: ดร.อดิสร เตือนตรานนท์, 113 หน้า.

การใช้สารเคมีที่น้อยลงและลดการผลิตของเสียในระบบจุลภาคเป็นหนึ่งในแนวทางของเคมีสีเขียว จึงได้เกิดแนวคิดในการพัฒนาระบบของไหลจุลภาคสำหรับการตรวจวัดแคลเซียมโดยใช้หลักการ Arsenazo III ขึ้น ด้วยวิธีการนี้ ได้มีการออกแบบสิ่งกีดขวางรูปตัวเจจำนวน 4 ชุด ชุดละ 10 ชิ้น ภายในท่อขนาดเล็กเพื่อช่วยในการผสมกันของสาร ซึ่งพบว่ามีประสิทธิภาพการผสมของสารประมาณ 90 เปอร์เซ็นต์ และเมื่อนำมาตรวจวัดหาปริมาณแคลเซียม ปฏิกิริยาที่เกิดขึ้นนี้สามารถวัดด้วยไฟเบอร์ออฟติกสเปคโตรมิเตอร์ที่ความยาวคลื่น 650 นาโนเมตรได้โดยตรง โดยระบบที่พัฒนานี้สามารถทำการตรวจวัดปริมาณแคลเซียมได้ในช่วงความเป็นเส้นตรง 0.2 - 3 mg dL^{-1} ค่าต่ำสุดที่สามารถวัดได้คือ 0.138 mg dL^{-1} วิธีที่พัฒนาขึ้นนี้มีความแม่นยำในการวิเคราะห์ปริมาณแคลเซียมสูง เมื่อทำการวิเคราะห์ปริมาณแคลเซียมระดับต่ำและสูง (within-run CV = 4.10% และ 3.91% ตามลำดับ, run-to-run CV = 4.6%) ผลกระทบจากการ carry-over ของสารมีค่าเท่ากับ 1.98% ซึ่งอยู่ในเกณฑ์ที่สามารถยอมรับได้ ผลการตรวจวัดปริมาณแคลเซียมในเลือดด้วยระบบที่พัฒนาขึ้น เทียบกับวิธีวิเคราะห์อัตโนมัติที่ใช้ในห้องปฏิบัติการทั่วไป ที่ใช้หลักการสเปคโตรโฟโตมิทรี พบว่ามีความสัมพันธ์ที่ดีสอดคล้องกัน (r^2 = 0.985; n= 15) ผลงานวิจัยแสดงให้เห็นว่าระบบของไหลจุลภาคที่พัฒนาขึ้นนี้ สามารถวิเคราะห์หาปริมาณแคลเซียมในเลือดได้และสามารถลดปริมาณการใช้สารเคมีลงได้อย่างมาก

ภาควิชา เคมีคลินิก	ลายมือชื่อนิสิต .....
สาขาวิชา ชีวเคมีคลินิกและอณูทางการแพทย์	ลายมือชื่อ อ.ที่ปรึกษาวิทยานิพนธ์หลัก .....
ปีการศึกษา 2553	ลายมือชื่อ อ.ที่ปรึกษาวิทยานิพนธ์ร่วม .....

5177217137 : MAJOR CLINICAL BIOCHEMISTRY AND MOLECULAR MEDICINE
KEYWORDS : ARSENAZO III / CALCIUM DETERMINATION / PORTABLE MICROFLUIDIC SYSTEM / PASSIVE MICROMIXER

YUWADEE BOONYASIT : PORTABLE MICROFLUIDIC SYSTEM FOR DETERMINATION OF CALCIUM BASED ON ARSENAZO III METHOD.
ADVISOR: ASST. PROF. WANIDA LAIWATTANAPAISAL, Ph.D.
CO-ADVISOR: ADISORN TUANTRANONT, Ph.D., 113 pp.

The ability for low reagent consumption and minimum waste production in a miniaturised system has generated great interest in the green chemistry field. Herein, a microfluidic system for calcium assays using the arsenazo III method has been developed. Using this approach, our proposed design, four sets of 10-piece J-shaped baffles within the microchannel, can strongly encourage chaotic flow of two different fluids. A homogeneous mixing (~ 90% homogeneity) was attained in a short time and within a limited length. The reaction between arsenazo III and calcium to form a blue-purple coloured complex was measured by an embedded miniature fibre optic spectrometer through absorbance increments at 650 nm. A linear range was obtained from 0.2 to 3 mg dL^{-1} with a detection limit of 0.138 mg dL^{-1} (S/N=3). The method exhibited good reproducibility based on low and high calcium tests with control serums, the within-run coefficient of variation (CVs) (4.10% and 3.91%), and the run-to-run CV (4.6%) were obtained. The carry-over effect of the method was 1.98%, which is acceptable for the current system. When compared to a conventional spectrophotometric method, this portable, microfluidic method correlated highly when evaluating serum samples (r^2 = 0.985; n= 15). This apparent similarity suggests that our proposed system could be used for determining the amount of calcium in serum samples.

Department : Clinical Chemistry Student's Signature .....
Field of Study : Clinical Biochemistry and Molecular Medicine Advisor's Signature .....
Academic Year : 2010 Co-advisor's Signature .....

ACKNOWLEDGEMENTS

I owe a huge debt of gratitude to my principal advisor, Asst. Prof. Dr. Wanida Laiwattanapaisal, who has always encouraged and supported me during my study on undergraduate and graduate degree. As a matter of fact, she is not only like a mother to me, but also a highly revered mentor. I particularly wish to thank Dr. Adisorn Tuantranont, my co-advisor, for providing expert guidance and excellent support, and for introducing me to the microfluidics. With his constant encouragement, it makes me work under him a pleasurable experience.

I would like to extend my thanks to all the research staff of Nanoelectronics and MEMS Laboratory, especially Thitima Maturos, Apichai Jomphoak, and Assawapong Sappat, for her help with cleanroom processing, his guidance on computational simulation, and his attempt to construct an in-house temperature controller, respectively. All my colleagues at the Department of Clinical Chemistry are recognised for their continuous support and warm friendship. I have found the contentment for working with these individuals. For being a part of my committees and their valuable time, I feel a deep sense of gratitude to Assoc. Prof. Dr. Rachana Santiyanont, Assoc. Prof. Dr. Mana Sriyudthsak, and Dr. Wijitar Dungchai.

I am deeply indebted to the Thailand Graduate Institute of Science and Technology scholarship (under the contract no. TG-44-09-51-094M), the CU Graduate School Thesis Grant, and the financial support for Master's students to present academic papers in a foreign country from Graduate School.

Lastly, and with no less gratitude, I would like to express my appreciation to my parents, Pol. Lt. Col. Somkiat and Jamsai Boonyasit, for being supportive and encouraging. Any merit of this thesis, I wish to dedicate this work as a token of my indebtedness to my parents and all my revered mentors.

CONTENTS

CHAPTER Page

CHAPTER Page

LIST OF TABLES

LIST OF FIGURES

Figure Page

Figure Page

CHAPTER I
INTRODUCTION

1. Introduction

In human body, about 99% of calcium is made up of bones and teeth. The remaining 1% is found in blood circulation and other extracellular fluids [1]. Approximately 50% of blood calcium exists in ionic form, while other types are bound to proteins and anions. The calcium ion plays an important role in blood coagulation, neuromuscular conduction, maintenance of membrane function, intracellular regulations of glandular secretion, and control of skeletal and cardiac muscle contractility [2]. Increased calcium levels in serum are reported in hyperparathyroidism, metastatic bone lesions, and hypervitaminosis, whereas decreased levels are observed in hypoparathyroidism, nephrosis, rickets, steatorrhea, nephritis, and calcium-losing syndromes [3]. In other words, the determination of calcium levels is very useful for clinical diagnosis.

There are two common approaches for the quantitative analysis of calcium ions. The first technique involves instrumental analysis, such as atomic absorption spectroscopy (AAS) and ion-selective electrode methodology. The second relies on specific dye binding methods. AAS is recommended as the reference method for ionised calcium assays; however, AAS requires expensive and sophisticated instruments [4-5]. Comparatively, ion-selective electrode methods require air exclusion from the sample to acquire accurate measurements [6]. Based on these restrictions, total serum calcium has become the method of choice for most

laboratories. This method is easy to perform and offers an accurate interpretation at clinically significant levels.

Specific dye binding methods, such as methylthymol blue [7], *o*-cresolphthalein complexone (CPC) [8-9], and arsenazo III [10-12], are used for determining total calcium levels because of their rapidity, convenience and inexpensiveness. However, the method utilising methylthymol blue suffers from dye instability in an aqueous solution [13]. Therefore, the reagent kit must contain two separate compositions. Similarly, the CPC reagent compositions, including an acidic colour reagent and an alkaline reagent composition, also need to be prepared separately [14]. The disadvantage of these multi-reagent methods is the complexity of each assay. On the other hand, arsenazo III, a dye that specifically binds calcium to form a complex, can be prepared and used as a single assay reagent [11]. Consequently, the arsenazo III method has become more popular. Nevertheless, arsenazo III is an organic, arsenic compound that contributes to environmental problems. Because the goal of green chemistry is to minimise reagent consumption and waste production [15], one possible solution to this problem involves microfluidic-based platforms. Therefore, by combining a microfluidic system and the arsenazo III method, a reduction in arsenic's environmental effect should occur.

The movement of clinical diagnostics towards microfluidics has begun to emerge because microfluidics offer many advantages, such as low reagent consumption, short reaction times, low waste product, and portability [16-17]. Many of microfluidic devices have been carried out in PDMS, which is flexible, transparent, and inexpensive [18-19]. Moreover, it is compatible with biological studies and many optical detection methods, particularly absorbance detection. Up until now, the

measurement of on-chip absorbance for clinical diagnoses has continued to develop [20-22]. Due to the portability of optical-fibre system, it is suitable for near-patient devices used at the hospital bedside. However, the short optical path length and the difficulties in coupling the light into and out of microchannels are still the main problems [23]. To overcome these limitations, the custom-made flow cell with a 1-cm path length incorporated into microchip was developed by our group [24-25].

Recently, there have been several reports describing microchip-based systems for calcium assays. For example, Malcik et al. [22] proposed a microchip-based fibre optic detection system for determining calcium ions levels in urine. The arsenazo III method was coupled with reflective measurements and the sensitivity of the calcium assay was noticeably improved. In a related study, Caglar et al. [26] proposed a glass-poly(dimethylsiloxane) (PDMS) microchip sensor for measuring calcium levels in serum; this technique exploited the reflective analysis of arsenazo III immobilised polymer beads.

For this study, a portable microfluidic system based on the arsenazo III method was configured for assaying calcium. Arsenazo III reacts with calcium to form a blue-purple coloured complex, which is measured by the integrated miniature fibre optic spectrometer with a 650-nm absorbance increment. In microfluidic-based biochemical analysis, homogeneous mixing is crucial for most bio-analytical systems to obtain high sensitivity and good reproducibility. Typically, with the small dimensional channel of a microchip, complete mixing will only occur when the two fluids are dispersed with each other in the decimetre lengths of a microchannel [27-29]. As a result, micromixer designs for integration into Lab-on-a-chip (LOC) technology have made great strides to reduce the need for long mixing lengths [30-

31]. Passive, planar micromixers utilising various obstacles for fluidic and particle mixing, have became an alternative approach [32-33]. They can be easily fabricated and integrated into microfluidic systems.

In our study, the J-shaped obstacles were modified to exaggerate the mixing effect; four sets of 10-piece baffles were introduced within the main microchannel. Herein, a computational simulation was performed with our micromixer, and its mixing results were compared with those obtained from an experimental fluorescence technique. The two approaches showed similar results, which indicated the versatility of the proposed passive micromixer and supported its possible integration into a LOC system. Moreover, the applicability of the micromixers for serum sample analyses with calcium evaluated the effectiveness of the proposed system.

2. Objectives

1. To design, fabricate, and characterise the passive micromixer for integration into Lab-on-a-chip technology.

2. To develop the portable microfluidic system for determination of total calcium.

3. To demonstrate the versatility of the proposed system by assaying calcium in real serum samples.

4. To decrease the reagent consumption and toxic waste products corresponding to the concept of green chemistry.

CHAPTER II
LITERATURE REVIEW

1. Calcium and hormonal control of its metabolism

In human body, calcium is the most abundant mineral and the most prevalent cation found in the body. Approximately 99% of calcium is made up of bones and teeth, whereas the remaining 1% is found in blood circulation and other extracellular fluids [1]. In the plasma, about 50% of blood calcium exists in ionic form, while other types are bound to plasma proteins (mainly albumin) and anions. Virtually all of the calcium in plasma has a concentration in the range of 8.6 to 10.2 mg dL^{-1} [34], which depends on the balance between intake and loss. The changes in blood pH directly affect the binding of calcium and protein. In alkalosis, the level of calcium bound protein increases, whereas the ionised calcium decreases. Conversely, when the blood pH decreases, it causes a decrease in calcium-bound protein and an increase in free calcium ions [6]. Due to these inverse relationships, the specimen collection should avoid the alterations in pH.

Typically, calcium homeostasis is relied heavily on the level of circulating calcium that involved in three principal organs, i.e. the small intestine, the skeleton, and the kidneys. Under normal physiologic conditions, the dietary calcium can be absorbed by the small intestine and rapidly cleared through the glomeruli of kidneys. In order to keep a balance between blood calcium circulation and potential reservoir of calcium, the skeleton can release the stored calcium to the blood; conversely, a high level of blood calcium can be stored in bone. Based on these mechanisms, the free calcium ions are physiologically active and maintained by the calcium regulating

hormones, i.e. parathyroid hormone (PTH), and 1,25-dihydroxyvitamin D (active form of vitamin D) [35]. These two primary hormones play the principal roles in the control of blood calcium, whereas the physiological role of calcitonin is uncertain [6]. As shown in Figure 1, the parathyroid glands secrete the parathyroid hormone in response to the hypocalcemia; on the contrary, the hypercalcemia inhibits the PTH secretion. PTH has major effects on both bone and kidney. In the bone, PTH activates osteoclasts activity, which breaks down bone and subsequently releases calcium into the extracellular fluid (ECF). By contrast, PTH conserves calcium by increasing tubular reabsorption of calcium ions and also stimulates the renal production of 1α-hydroxylase [36]. Based on this secretion of renal enzyme, the 25-hydroxy vitamin D, the main circulating form of vitamin D, is metabolised to 1,25-dihydroxy vitamin D [3]. Then, the active form of vitamin D increases calcium absorption in the intestine and enhance the renal reabsorption of calcium. In order to continue the blood calcium to be maintained in the normal range, the active vitamin D feeds back on the down regulation of PTH secretion.

Up until now, although the physiological control of calcitonin secretion is still not well understood, its action inhibits the osteoclast activity. There have been reported that calcitonin can decrease the serum calcium and phosphate concentrations when taking high pharmacological doses [37-38]. The C cells of thyroid gland produces the calcitonin; therefore, the increased circulating concentrations of calcitonin have been associated with the medullary thyroid carcinoma (MTC) or nonthyroidal malignancies [35].

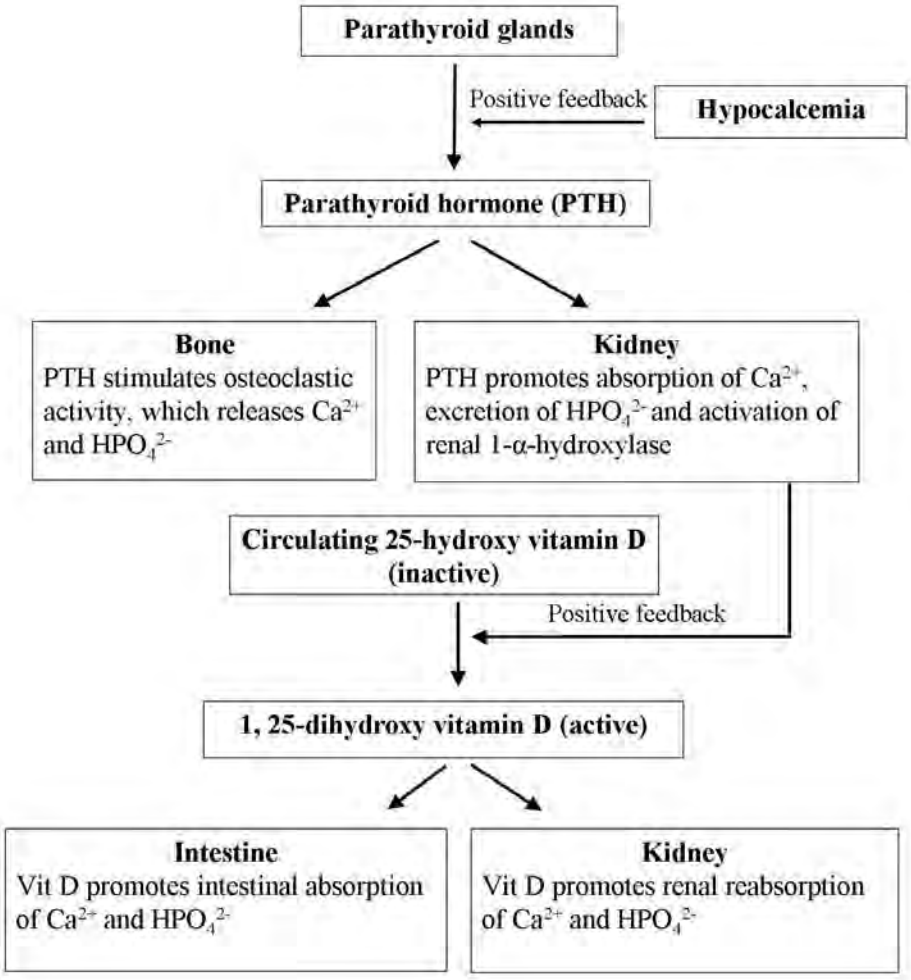

Figure 1. Integrated control of calcium homeostasis [1].

1.1 Disorders of calcium metabolism

As well known, the intracellular calcium ions play an important role in muscle and nerve function, whereas the extracellular calcium ions are involved in bone homeostasis and blood coagulation [2]. Consequently, the quantitative measurement of calcium is determined for monitoring the diseases of bone or calcium regulation disorders. As listed in Table1, the dramatic changes in calcium levels are associated

with a large number of disease states. The common cause of hypercalcemia is closely related to the primary hyperparathyroidism and malignancy, whereas the leading cause of hypocalcemia is associated with the critically ill patients. The abnormalities in acid-base regulation and losses of protein, i.e. chronic liver disease, acute pancreatitis, nephrotic syndrome can contribute significantly to hypocalcemia. Also, primary hypoparathyroidism and vitamin D deficiency can result in the decreased calcium levels. Although the clinical signs and symptoms of hypercalcemia are nonspecific, the abnormalities in neuromuscular system can be present at the high concentrations of calcium. In the case of hypocalcemia, the most common signs and symptoms are tetany, seizures, paresthesia and hypertension [35].

Table1. Causes of hypercalcemia and hypocalcemia [1, 6, 39]

Hypercalcemia	**Hypocalcemia**
Primary hyperparathyroidism– adenoma or glandular hyperplasia	Primary hypoparathyroidism– glandular aplasia, destruction, or removal
Hyperthyroidism	Hypomagnesemia
Malignancy	Hypoalbuminemia– chronic liver disease, nephritic syndrome, malnutrition
Multiple myeloma	Acute pancreatitis
Benign familial hypocalciuria	Vitamin D deficiency
Increased vitamin D	Renal disease
Thiazide diuretics	Rhabdomyolysis
Prolonged immobilization	Pseudohypoparathyroidism

2. Calcium determination

As mentioned earlier, serum calcium determination is an extremely important test for clinical diagnosis. The changes in calcium level are associated with numerous illnesses, especially the diseases of bone or calcium regulation disorders. For this reason, several approaches have been developed for monitoring the calcium level in serum. Normally, calcium can be classified into three forms: ionised calcium, protein-bound calcium, and complex calcium. The total calcium is the combination value of ionised calcium, protein-bound calcium, and complexed calcium. Thus, the development of method for assaying calcium depends on the calcium forms found in serum. In this case, ionised calcium is usually determined by using atomic absorption spectroscopy (AAS) and ion-selective electrode method, whereas the total calcium is quantified by specific dye binding methods. The common approaches for the quantitative analysis of calcium are described in detail as listed below.

2.1 Potentiometric sensors

Ion-selective electrode method (ISE), which is categorized into two types: direct and indirect ISE, is valuable to determine the free calcium ions. The direct ISE is based on the direct analyzed sample, whereas the indirect ISE depends on the acidic diluents for diluting the sample before measurement. Basically, the combination of two different electrodes is involved in the ISE technology: a reference electrode and an ion selective electrode. When the electrodes come into contact with the calcium ions, the potential across the membrane can take place and the action potential is directly proportional to the amount of calcium. The conventional ISE, or so called the indirect ISE, is generally relied on the measurement of ionised calcium. Using this

approach, the acidic diluent is used to convert protein-bound and complexed calcium into free calcium ions before analysis an amount of calcium in samples. According to the United States Patent number 5,424,214, Shu et al. [40] proposed the indirect potentiometric determination of total calcium in clinical samples utilising the strongly acidic diluents. They demonstrated the appropriate composition of diluents including the preservatives and surfactants for measuring the calcium concentration, and the effective volume to volume ratio of the clinical samples to the diluent.

2.2 Utilizing enzymatic reaction for quantitative determination of calcium

In the earlier decade, many researchers had turned their attention to develop a reagent for quantitative determination of calcium ions by using the benefit of enzymatic reaction. For example, apo-type transglutaminase [41] and phospholipase [42-43] were employed as an analytical composition of reagent for measuring the calcium level in clinical samples. According to the United States Patent number 5,618,684, Nonobe et al. [41] disclosed the method for determining the amount of calcium in samples by monitoring the transglutaminase activity. Apo-type transglutaminase (EC 2.3.2.13) is highly specific to calcium and its activity depends on the amount of calcium. When calcium brings into contact with transglutaminase, it can activate the transglutaminase activity. Then, the activated transglutaminase acts with its substrates and the production of ammonia will increase. Consequently, the amounts of generated ammonia are correlated with the level of calcium in blood samples. In another approach, the method for quantitative analysis of calcium comprising the phospholipase enzyme has been proposed [42-44]. Typically, the phospholipase enzyme including phopholipaes A_1 (EC 3.1.1.32), phopholipase A_2

(EC 3.1.1.4), and phospholipase D (EC 3.1.4.41) can hydrolyze a phospholipid. The substrates and reaction products of phosphalipase A_1, A_2 and D are summarised in Table 2. In addition, the methods for measuring the amount of a reaction product are summarised in Table 3. Based on the benefit of phosphalipase enzyme, Mihara et al. [42] disclosed the method of using a compromise between phospholipase D and choline oxidase. Their proposed method could determine the amount of calcium over a broad range of concentration. The principle of calcium assay based on the reagent comprising a phospholipase D and a choline oxidase enzyme is illustrated below.

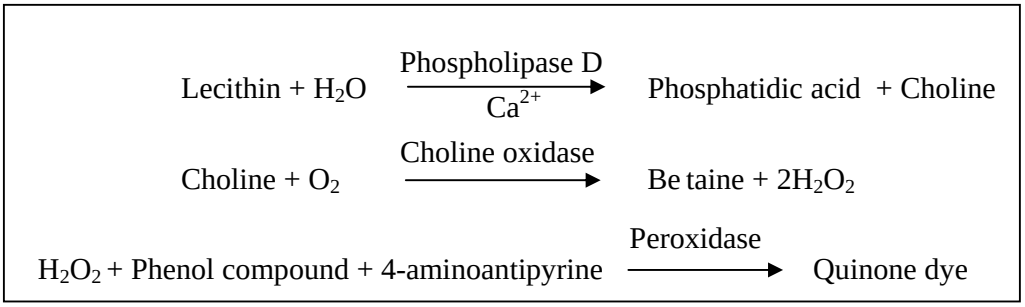

Table 2. Substrate and reaction product of phospholipase A_1, A_2, D [43]

Substrate	Enzyme	Product
Phosphatidylcholine Phosphatidylglycerol Phosphatidylethanolamine	Phospholipase A_1 Phospholipase A_2	Acetic acid Fatty acid
Phosphatidylcholine Phosphatidylglycerol Phosphatidylethanolamine Phosphatidylinositol Phosphatidylserine	Phospholipase D	Choline Glycerol Ethanolamine Inositol Serine

Table 3. Method for measuring the amount of reaction product of phospholipase A_1, A_2, D

Substrate	Enzyme	Product	Ref.
Acetic acid	Alcohol dehydrogenase	NADH	[45]
Glycerol	Glycerol oxidase	Glyceraldehyde + H_2O_2	[46]
Glycerol + ATP Glycerol-3-phosphoric acid + NAD	Glycerol kinase Glycerophosphate dehydrogenase	Glycerol-3-phosphoric acid NADH	[46]
Ethanolamine	Ethanolamine oxidase	Glyceraldehyde+ ammonia + H_2O_2	[47]
Serine	Serine dehydrogenase	Pyruvic acid + ammonia	[48]

2.3 Specific dye binding methods

As being stated on the Tietz Fundamentals of Clinical Chemistry 2008, approximately 75% of clinical laboratories exploited the spectrophotometric method and almost 24% of laboratories used ion-selective electrode method for the measurement of calcium level [35]. By using spectrophotometric method, the metallochromic indicators have become a method of choice because they are easy to perform. More recently, the frequency used metallochromic dyes for determining total calcium levels are *o*-cresolphthalein complexone (CPC) [8-9, 49-50] and arsenazo III [10-11, 51-52].

.

2.3.1 *O*-cresolphthalein complexone (CPC)

In accordance with dye binding method, CPC reacts with calcium to form a bluish-purple coloured complex under the alkaline condition, which can be measured by the spectrophotometer at a wavelength of 570 nm. With this approach, the acidic colour reagent and alkaline reagent composition are prepared separately due to the dye instability [14]. The reagent stability is limited by the absorption of carbon dioxide (CO_2) [53]. Besides being unstable, the CPC method does not bound to albumin-bound calcium completely because of its stoichiometry [44]. In addition, magnesium ions can bind to arsenazo III reagent under the alkaline condition; thus, hydroxyquinoline-5-sulphonic acid (8HQS) is required to be a masking agent [52].

2.3.2 Arsenazo III

Arsenazo III is selected for determination of serum calcium because it provides high sensitivity, high affinity, and ability to form a stable colour complex with calcium over a wide pH range [11, 54]. The intensity of the colour formed is directly proportional to the amount of calcium present in the sample. Owing to a single stable reagent, the arsenazo III method has become more popular. In this case, Leary et al. [11] disclosed the single-reagent method for calcium measurement in serum and plasma with the use of arsenzo III. With this approach, the reaction proceeded under slightly acidic conditions. Their proposed method exhibited the good agreement with results from AAS technique and the analytical curve was linear from 0 to 5 mM. A few years later, Morgan et al. [12] proposed the stable alkaline-reagent for calcium determination in serum. Their analytical procedure included a triglyceride clearing technique and a magnesium-masking agent in the reagent. When comparing

the results obtained from their proposed method with those from an acid arsenazo III-based reagent, the results implied that both methods were highly correlated. Up to the present day, Malcik et al. [22] demonstrated the use of arsenazo III in microchip-based detection system. Due to the maximum absorbance at the pH of 9, they selected the sodium hydroxide/boric acid mixture solutions for their subsequent experiments. The linearity of calibration curve was obtained in the range of 0.125-2.5 mM with the detection limit of 0.085 mM. Apart from this, the continuous improvement on calcium assay is shown in Table 4 with its pros and cons of using various means.

Arsenazo III is an organic arsenic compound having the structure formula as shown in Figure 2. Even though arsenazo III is highly sensitive and specific for calcium, it can cause the environmental problems. In order to overcome these limitations, the microfluidic system promises to be an alternative approach. By using this microfluidic-based platform, it can minimise the reagent consumption and waste production; therefore, a reduction in arsenic's environmental effect can be achieved.

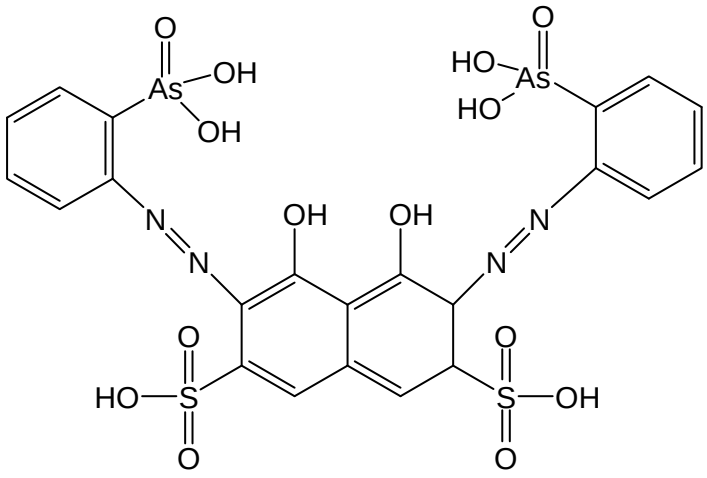

Figure 2. Structure of arsenazo III

Table 4. Pros and cons of using different procedures for calcium determination

Principle	Pros	Cons	Year	Ref.
Atomic Absorption Spectrophotometer (AAS)	➢ Accuracy ➢ Reference method	➢ Need sophisticated & expensive instrument ➢ Sample dilution	1967	[55]
Methylthymol blue	➢ No dialysis ➢ Stable acidic solution	➢ Two separate aqueous solution	1973	[13]
Phthalein purple	➢ Easy to handle ➢ Long shelf life	➢ Protein precipitation	1974	[56]
Murexide (titrimetric determination)	➢ Stable reagent	➢ Difficult to prepare an alkaline murexide	1974	[57]
o-cresolphthalein complexone (CPC)	➢ Eliminate the use of diethylamine (offensive odor & hazard)	➢ Two separate aqueous solution ➢ Need 8-HQ	1976	[14]
Arsenazo III	➢ Single & stable reagent ➢ Simple & economical	➢ Arsenic toxicity	1991	[51]
Arsenazo III	➢ Single & stable reagent ➢ Triglycerides clearing	➢ Arsenic toxicity	1993	[52]
Ion selective electrodes (Potentiometric method)	➢ Total calcium determination	➢ Indirect potentiometric method (sample dilution)	1995	[40]

Principle	Pros	Cons	Year	Ref.
Enzymatic determination (transglutaminase)	➢ No pretreatment ➢ Rapid & accurate determination ➢ High specificity	➢ Platelets contain coagulation factor III (transglutaminase group)	1997	[41]
Enzymatic determination (phospholipase D,choline oxidase)	➢ Accurate determination ➢ Wide range of calcium concentrations ➢ Easy to prepare	➢ Unsuitable for continuous measurements ➢ Influence on co-present salts	1999	[42]
Enzymatic determination (Phospholipase D and BPNPP)	➢ Simple and specific enzymatic assay	➢ Need tartaric acid and sodium sulfate	2005	[44]
Chlorophosphonazo III	➢ No arsenic toxicity ➢ Suitable for weakly acidic ➢ No problem of carbonic acid gas absorption ➢ Low blank values ➢ Good storage stability	➢ Two reagent system ➢ Need vanadate ions	2006	[58]
Chromoionophores	➢ Using standard instrument (UV-Vis spectrometers)	➢ Wet storage stability	2007	[59]

3. Microfluidics or Lab-On-a-Chip Technology

Lab-on-a-chip technology appears to be a miniaturised laboratory on a small microfluidic device, which consists of microchannels, valves, mixers, reaction chambers, pumps, electrodes and sensors [60]. Such devices provide several benefits. For example, they use a much smaller volume of sample and reagent than conventional techniques. Therefore, they are cheaper, quicker, less hazardous to use and more environmentally appealing [16-17]. Additionally, many researchers nowadays have turned their attention to the concept of green chemistry or so-called clean chemistry [15]. This burgeoning field is focused on the environmental pollution and human hazards. Based on the concept of a safe environment, the chemical processes that minimise or eliminate the toxic waste have become manifest in microfluidic systems.

3.1 Micromixers

Due to the small dimension of microfluidic channels, the diffusion becomes the primary mixing mechanism for achieving the homogeneous mixing of two different fluids [30-31]. In this case, the complete mixing will occur in a long length of microchannels. Thus, there is a need to design the micromixers to exaggerate the mixing performance in a short time and within a limited length. As shown in Figure 3, the classification of micromixers was described in detail by Nguyen et al. [30]. The most common micromixers are categorised into two major groups: active and passive mixers. Based on active mixers, they require the external force to introduce the mixing in the microchannels such as electrohydrodynamic [61], electrokinetic [62], ultrasonic [63], magnetic [64], and thermal driven mixers [65]. These mixers

offer many advantages over the passive mixers that they can perform better in time. Nevertheless, the main drawback of these mixers is unsuitable for biological samples such as whole blood and cell suspensions. The ultrasonic wave and high temperature can damage these biological samples [63]. To overcome this limitation, the passive micromixers have become an alternative approach [33].

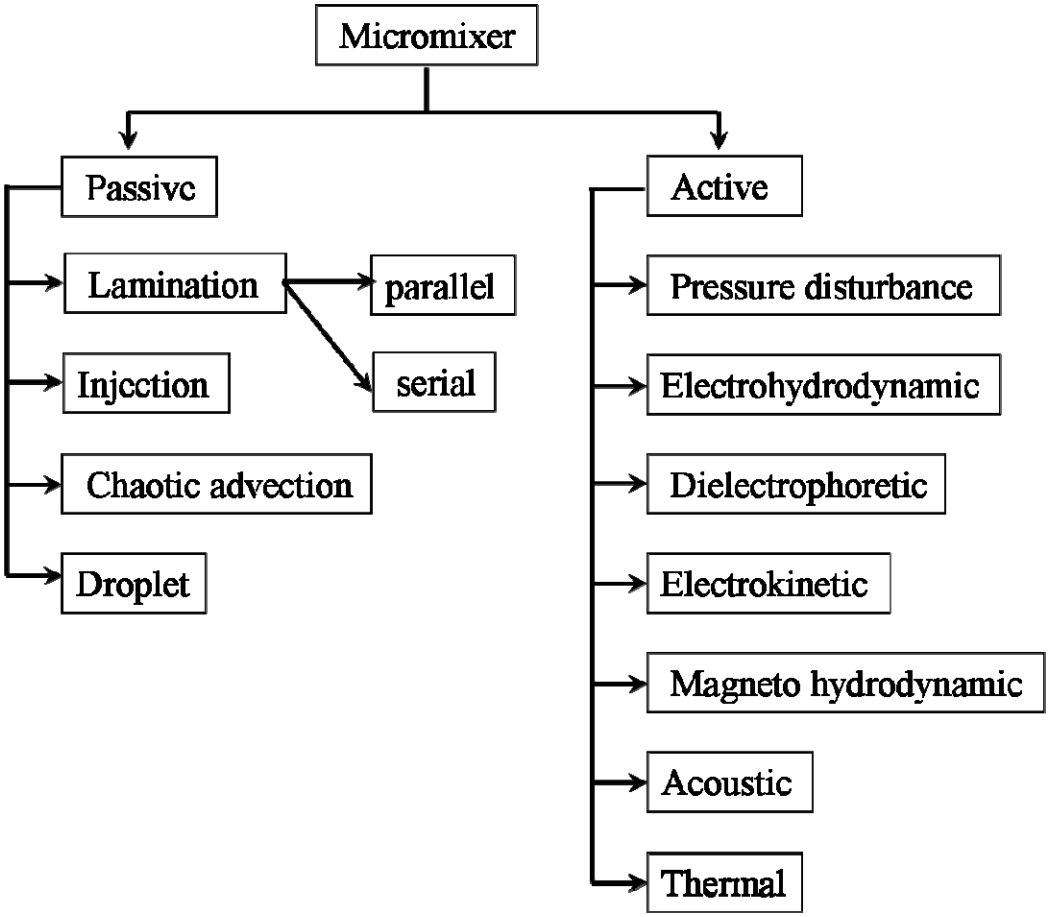

Figure 3. Classification of micromixers (Modified from Nguyen et al. [30]).

Passive, planar micromixers utilise the channel geometry to combine the two different fluids. They can be easily fabricated and integrated into the microfluidic systems. Additionally, there is no need for applying the external force to these mixers. Serial lamination [66-67], parallel lamination [68-69], interdigital multi-lamination [70-71], injection [72], chaotic advection [73-76], and droplet [77-78] are examples of mixing mechanisms used in passive mixers. Based on chaotic advection, the mixing is achieved by introducing the obstacles within channels or by modifying channel geometries. Many designs have been reported in the literature [75, 79-83]. For example, Jen et al. [80] proposed the investigation of twisted microchannel with three different designs: inclined; oblique; and wavelike mixer. Their results demonstrated that the micromixer with the inclined channel could improve mixing. By comparison with the basic T-mixer, this design could decrease the mixing length up to 31%. Apart from this, the other chaotic micromixers using two-layer crossing channels were designed by Xia et al. [75]. Their two models exhibited excellent mixing performance at low Reynolds numbers. The chaotic advection was generated through the continuous stretching, folding and splitting, and reorientation and recombination. When compared to the single twisted or serpentine channel, these designs did not rely on the fluid inertial effects and provide the rapid mixing at low Reynolds numbers. However, the twisted microchannels and two-layer crossing channels were complex to fabricate due to their three-dimensional structures. Also, the precision multilayer alignment between three-dimensional channels was difficult. For these reasons, a planar two-dimensional structure of micromixer has become a method of choice. A new micromixer type, which combined curved channels, split-and-recombine structures, and flow separation was proposed by Mouza et al. [81]. Their findings

reported that the simple planar meandering channels could induce chaotic advection. Another approach based on a planar micromixer with rhombic microchannels and a converging-diverging element was recommended by Chung et al. [79]. Additionally, Tsui et al. [82] indicated that the grooved and obstructed channels could enhance the mixing performance. The different geometries of microchannels were also investigated by Hossain et al. [83]. Their works presented a numerical investigation on the three different geometries of microchannels, i.e. zig-zag, square-wave, and curved. The square-wave microchannel exhibited the best mixing performance. In contrast, the square-wave and zig-zag microchannels provided the higher pressure drop than the curved microchannel due to the sharp turn of channel geometries. Their findings could be concluded that the important characteristics while designing the passive micromixers were the compromise between the mixing performance and pressure drop.

As mentioned above, passive mixers are relatively simpler to fabricate and easier to integrate with Lab-on-a-chip technology. Therefore, there is a great need to develop better passive mixers for complete microfluidic systems. Several key designs are summarised in Table 5.

Table 5. Summary of key passive microfluidic mixer designs

Principle	Cross-section HxW (μm)	Re	Mixing Length (mm)	Material	Remarks	Ref.
Serpentine	150x300	6-70	3.6-9	Si-glass	➢ Complex 3-D fabrication	[84]
Chaotic advection	150x250	936	182.4	PDMS	➢ Long length	[85]
Chaotic advection	150x300	0.01-0.2	5.73	PMMA	➢ Complex 3-D fabrication	[75]
Chaotic advection	38900x 10600	< 1	32	PDMS	➢ Capillary force	[86]
Chaotic advection	85x200	0.001-10	5-15	-	➢ Staggered herringbone mixer	[87]
Chaotic advection	100x300	0.08-16	7.4	PDMS	➢ Complex 3-D fabrication	[88]
Chaotic advection	500x500	20-350	7	PDMS	➢ High pressure drop	[81]
Chaotic advection	77x200	0.01-10	10-17	PDMS	➢ Complex 3-D fabrication	[74]
Chaotic advection	60x240	0.288-2.88	10-20	PDMS	➢ Complex 3-D fabrication	[73]
Coanda effect	90x200	70	7	COC	➢ Mixing can damage biological samples	[89]

3.2 Fabrication of microfluidic device

Polymer-based method provides an effective alternative to chip fabrication process on account of being more amenable to mass production. A large number of replicas are generated from a single master, which can be fabricated by numerous techniques. The ways of producing a master such as laser micromachining [90], silicon micromachining (wet or dry etching) [91], and electroplating [92] are employed as a method of choice. Up until now, the replication technology is used in microfluidic systems due to its low manufacturing cost [93]. Based on this approach, the hot embossing, injection molding, and casting are a case in point [93-95]. The casting of PDMS has been received the great attention in the process of elastomeric microfluidic fabrication thanks to its simplicity of making up. To produce a replica, the liquid pre-polymer is simply poured over the master and cured, and then peeled it off.

Photolithography is an effective means of fabricating the silicon master [19]. To begin with, piranha etching is used for activating the silicon surface. Then, a photoresist is spun on the wafer and prebaked, as shown in Figure 4. Next, the photoresist-coated silicon wafer is exposed to UV light. After UV exposure, the developing reagent is used to dissolve the unexposed regions so that the exposed areas reveal the structure for microchannels. Eventually, the embossed microstructure is used as the master for cast replicas of PDMS. Using this approach, the widespread use of PDMS elastomers casting has still increased due to its flexibility and low cost in producing planar microchannel [18, 94]. The merits and demerits of PDMS properties are summarised in Table 6.

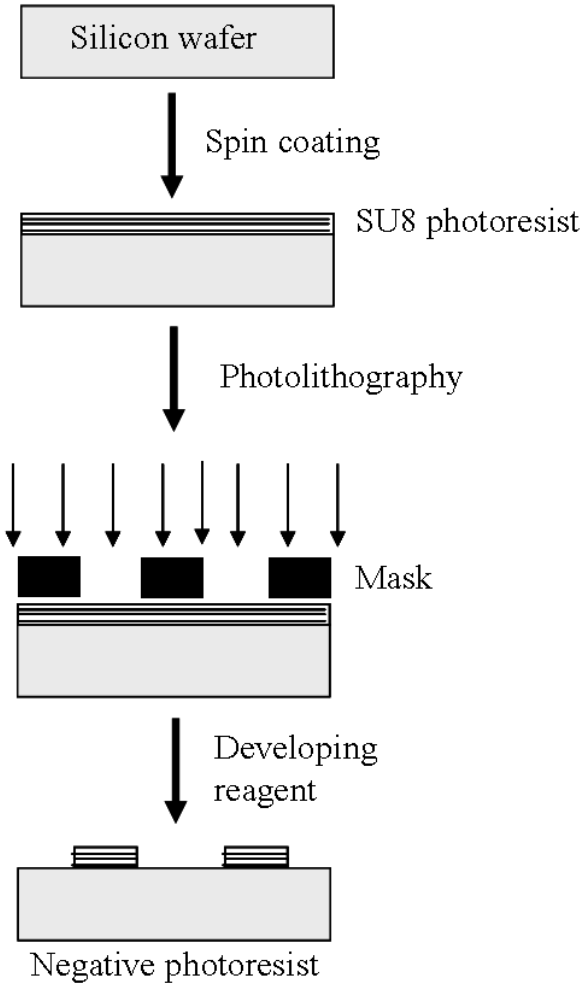

Figure 4. An illustration of the photolithography process. Silicon wafer was fabricated by using a negative relief of photoresist on its surface (Modified from Kane et al. [96]).

Table 6. Physical and chemical properties of PDMS [18, 96]

Pros	Cons
Optically transparent down to 280 nm	Hydrophobic
Very low fluorescence	High non-specific adsorption
Suitable for integrating optical gratings and waveguides into its surface	Poor wettability
Easy and rapid fabrication	Not optimal for mass fabrication
Reproducibility	Non-rigid
Covalent bonding with itself and other Si-based materials	-
Compatible with aqueous media	-
Excellent material for EOF and pressure pumping	-
Inexpensive	-
Non-toxic to cells and high permeability to gases	-

Although PDMS seems to be suitable for microfluidic applications, the high non-specific adsorption is still the main drawback of this silicone rubber. In order to overcome this obstacle to reduce the adsorption of hydrophobic analytes, Thorslund et al. [97-100] proposed the heparin coatings and instant oxidation of closed structures. Unless otherwise stated, PDMS brings the potential benefits of serving as smart materials for fabrication of microfluidic devices. In particular, the property of transparency is necessary for detection systems involving absorbance and fluorescence technique.

3.3 Determination of mixing efficiency

To date, there are two common approaches for evaluation of mixing capability, i.e. vibration analysis and flow visualization [31]. The first technique requires expensive and sophisticated instruments, such as IR, FTIR, and Raman spectrum analyses. In comparison to the first technique, the second is relatively simple to operate due to the visual evaluation, which comprises of a microscope, a high-speed camera, and a personal computer [27]. Hence, the flow visualization has become a method of choice for most current systems.

In the literature, many approaches have been employed as a mixing test [75, 79, 81, 86, 88, 101]. For example, Nguyen et al. [27] used the reaction between 0.5 M NaOH and 0.3 M phenolphthalein (in ethanol 99%) to test the quality of their proposed micromixer. Based on the liquid food dyes, Sudarsan et al. [102] have demonstrated their efficient mixing in planar spiral-shaped microchannel. Blue and yellow food dyes were utilised for their studies. When the two streams were mixed, the amount of green colour was generated. The alteration in colour of two different liquid food dyes indicated the mixing performance of their micromixer. In another approach, Chung et al. [79] have presented the rhombic micromixers comprising of three inlets. Ethanol, DI water, and 5 wt% deep blue ink were used as a model for quantification of mixing performance of three different fluids. They selected the deep blue ink (Quink co.) for their mixing purpose because the diffusion coefficient of this ink in water is close to that of ethanol in water.

For the stringent mixing test, a highly viscous glycerol solution was utilised by Xia et al. [75]. A 98% glycerol-2% liquid food dye (red and blue) solution was employed as a mixing test for their chaotic micromixers using two-layer crossing

channels. Due to the diffusive mixing of glycerol is very weak, the flow characteristics are only affected by the Reynolds numbers (Re). Their findings demonstrated that both of their designs did not rely on the fluid inertial effects, and chaotic advection still occurred at low Re. In a related study, the effect of different mixture viscosity of four unique liquids on mixing efficiency is also investigated by Mouza et al. [81]. They have developed the chaotic micromixer combining curved channel, split-and-recombine structures, and flow separation.

The change in pH values due to the reaction between acids and bases has been proposed for monitoring the mixing time. Majumdar et al. [101] demonstrated the reaction between a basic fluorescein dye (pH = 10) and an acidic buffer (pH = 3). In this case, the fluorescein solution was not fluorescent when the pH was lower than 4. Thanks to the dramatic change in intensity of two different fluids, the acid-base reaction was selected for their measurement of mixing time. With this approach, the time of complete mixing corresponded to the distance along the flow channel where the fluorescent signal reached the decrease in baseline values.

Using the fluorescence characterisation, Kim et al. [88] conducted an experiment on mixing efficiency by using the fluorescent images captured from the confocal microscope. To accomplish their purpose of achieving the efficient micromixer, they employed a three-dimensional microchannel structure for their mixing of confluent fluids. After utilising the successive mean filters, they assessed the mixing efficiency by the standard deviation of pixel intensities across the channel width.

In order to visualise the mixing tendencies by the naked eyes, Jeon et al. [86] demonstrated the use of gold nano-particles (Au NPs) and $CuSO_4$ solution for

assessing their mixing performance of passive micromixers with various geometric designs. The sudden changes in colour were brought about by the mixture of Au NPs and copper ions. Thus, they could observe the flow patterns of Au NPs aggregation based on a variation of colour.

As mentioned earlier, flow visualization has been an alternative approach to verify the mixing performance of two different fluids due to its simple matter [31, 103]. Using this approach, the quantitative measurement of mixing performance is important to represent the degree of uniformity. Thus, many researchers have made their attempts to succeed in assessing the degree of mixing efficiency [27, 88, 103-104]. The term, mixing index, which is the ratio of standard deviation to the mean of each cross section, was defined by Wu et al. [105]. However, up until now, it is hoped that the reliable and universal way to determine the quantity of mixing performance is called for.

3.4 On-chip absorbance detection

Nowadays, there is an increasing demand for clinical diagnostic systems utilising optical detection method [22, 26, 106-107]. For near-patient devices, the optical-fibre systems provide the great benefit for point-of-care diagnosis due to their portable platforms. Although the absorbance detection can be performed on-chip measurement as a single-step microfluidic device, the short path length in miniaturised systems can put limits on the sensitivity of these methods. In order to overcome this limitation, many researchers have attempted to increase the path-length of flow cell by using different geometric flow-cell such as Teflon tubing [108], PEEK

tube [109], silicone flow-cell [110], quartz flow cell [111], Z- or U-shaped capillary [112-113].

Recently, there have been several reports describing microchip-based systems for on-chip absorbance measurement. For example, Duggan et al. [108] demonstrated the liquid-core waveguide for on-chip spectrophotometric detection, utilising the Teflon fluoropolymers PTFE, FEP, and AF as cladding material. The overall design of liquid-core waveguides incorporating in microchip is illustrated in Figure 5. The results indicated that their system could increase the sampling path-length to 5 mm and provide the good reproducibility of crystal violet analysis. Another approach based on the optical sensor for determination of copper (II) by using micro flow system was proposed by Leelasattarathkul et al. [109]. A PEEK tube with 0.5 mm i.d. size is used as a flow cell (10 mm path length) for passing the solution. The light from a tungsten halogen lamp is carried to the flow cell and then directed to a spectrophotometre for measuring the absorbance. Their proposed system provided a satisfied sensitivity with a linear analytical curve over the range of 0.1-3.0 μg mL^{-1} of copper (II). In a related study, Kruanetr et al. [114] presented the implementation of the micro flow analysis (μFA) system for determination of iron in a polymethyl methacrylate (PMMA) microfluidic chip. The μFA flow cell (0.8 mm i.d., 10 mm path length), in which the complex of Fe (III)-nitroso-R salt was measured at 720 nm, was integrated with two fibre optic probes for absorbance measurement.

The feasibility of on-chip absorbance detection is a clear improvement on its integration into microfluidic systems. In this case, the new spectrofluorimetric and spectrophotometric microdetectors, designed for nano-volume sample measurements, have been proposed by Bargiel et al. [115]. They designed the C-shaped fluidic

channel for absorbance detection, as shown in Figure 6(A). The standard optical fibres were aligned in a horizontal position and the distance between the two fibres was 10 mm. Their works demonstrated the applicability of their systems by determining phosphate concentration in water. The results indicated the good sensitivity of phosphate determination with the linear range from 0.2 to 1.6 μg mL^{-1}. For the spectrofluorimetric detector, they designed the trapezoid-shaped channel for the sample flow cell. As depicted in Figure 6(B), the optical fibre (Fibre1) is aligned in a horizontal position of silicon chip, whereas another fibre (Fibre2) is positioned in vertical axis of the fluidic channel. When the sample is illuminated by an excitation light from fibre1, the fibre2 is used to collect the emitted fluorescent light. Their findings reported that the system provided a good sensitivity and reproducibility. The linear response was measured from 0 to 0.2 mg mL^{-1} of fluorescein and the peak wavelength of emitted fluorescent light (509 nm) was similar to the result obtained from the standard Fluka solutions (514 nm). In the same way, the liner analytical curve of erythrosine was in the range of 0-0.14 mg mL^{-1} with the comparable wavelength of spectrum peak.

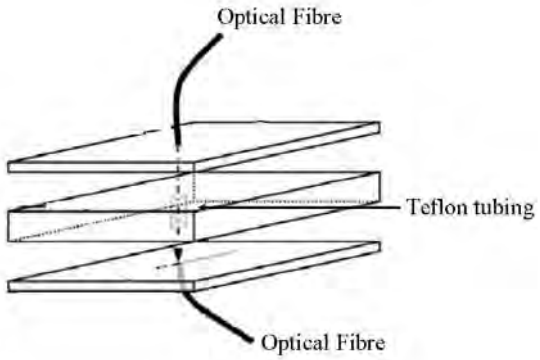

Figure 5. Configuration of optical fibres alignment and incorporation of Teflon based liquid-core waveguide in microchip (Modified from Duggan et al. [108]).

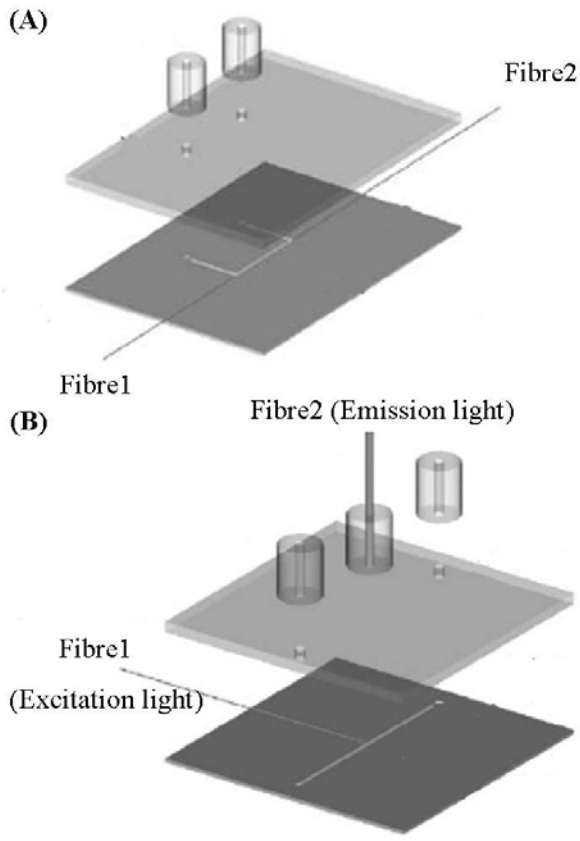

Figure 6. A diagram of optical fibres positions: (A) spectrophotometric detector; (B) spectrofluorimetric detector [115].

In regard to the clinical diagnoses, the on-chip absorbance measurement was utilised in testing the applicability of the microfluidic systems. More recently, Jindal et al. [116] performed on-chip electrochromatography for separation of three peptides. The experimental setup for on-chip UV absorbance detection was carried out. The standard cross channel is designed for electrochromatograpic purpose and fabricated in a quartz slide. The chromatographic chip is positioned between the two optical fibres connecting to the light source and detector. The results implied that the developed system could perform on-chip assay by using sol-gel technology as a particles packing stationary phrase. At the detection zone, the trapezoidal-shaped channel was constructed for using as an effective optical path-length. Additionally, another approach based on real sample analysis on chip was conducted. Malcik et al. [22] proposed a microchip-based fibre optic detection system for determining calcium ions levels in urine. An Ocean Optics USB2000 miniature fibre-optic spectrometer was exploited for their absorbance measurements. A single 400 μm UV-Vis fibres were used to transport light from the tungsten/halogen source. The arsenazo III method was coupled with reflective measurements and the sensitivity of the calcium assay was noticeably improved. Their linear range was found to be 0.125-2.5 mM with the detection limit of 0.085 mM. In a related study, Caglar et al. [26] proposed a glass-PDMS microchip sensor for measuring calcium levels in serum. This technique exploited the reflective analysis of arsenazo III immobilised polymer beads. In comparison to the previous work, the linearity of analytical curve provided a narrow range of calcium assay. Their linear range of the immobilised beads-based microchip was 0.0357-0.571 mM, with a limit of detection of 0.0268 mM.

3.5 Microfluidics for clinical analysis

In recent years, a sudden movement of clinical and biochemical analysis towards microfluidics has emerged as a distinct new field. The integration of multiples steps (sample preparation, injection, reaction, separation, and detection) into a single device is still challenging many researchers to think about these current issues. Generally, clinical tests are often performed on cell-free samples, such as serum or plasma, and urine. The centrifuge is required to remove blood cells from whole blood before assaying an analyte of interest. Thus, many researchers have turned their attention to overcome this limitation through the use of membrane filter incorporated onto a microfluidic device. In this case, Thorslund et al. [117] have developed the PDMS microdevice for on-chip whole blood filtration. Their proposed system consisted of a membrane filter sandwiched in-between channels of two different layers. With this device, the testosterone concentrations were measured with testosterone radio immuno assay (RIA). Another approach based on the incorporation of multiple steps into a single device is presented by Tan et al. [106]. They clearly demonstrated the detailed implementation of lab-on-a-chip based on optical detection of nerve agent sarin in whole blood. The potential use of their device depended on the continuous-flow with sequential stages, including the lysis of whole blood, regeneration step, protein precipitation, filtration, enzyme-assisted reaction, and optical detection. In the field of preventive medicine, Lien et al. [118] have proposed the miniature microfluidic system for detection of α-Thalassemia-1 deletion in saliva samples. Their system consisted of several integrated modules, i.e. a genomic DNA extraction module, a polymerase chain reaction module, and an external optical detection module. This saliva-based system could provide a promising platform for

rapid DNA extraction and detection of genetic diseases. Based on hematological screening test, Noda et al. [107] have demonstrated the applicability of absorption photometry microchip with long optical path length (5 mm) for hemoglobin measurement. With two 45° mirrors, the sensitive hemoglobin measurement was accomplished with stability in repetitive measurement. The results reported that the linear range of the proposed microfluidic system (3-20 g dL^{-1}) was covered with the normal range of human hemoglobin (12-17 g dL^{-1}). Thus, these findings can be implied that this microchip has an ability to be a hemoglobin screening test for the current use.

A state-of-the-art approach to cardiac markers screening is reported by Wolf et al. [119]. The combination of micromosaic immunoassays (μMIAs) and self-regulating microfluidic networks (μFNs) was employed to determine the cardiac markers, i.e. C-reactive protein (CRP), myoglobin (Mb), cardiac Troponin I (cTnI), and protein S100α. Due to a well-known and widely used marker of systemic inflammation, they selected CRP as a model. As well known, the clinically relevant concentrations of Mb and cTnI are the important indicators for prognosis of acute myocardial infarction (AMI). While Mb appears first after the onset of AMI, cTnI is a standard marker for the detection of AMI. Mb is found in blood circulation when the skeletal muscle or myocardial cells are damaged. Also, cTnI is a highly specific marker for damages of myocardium. Based on the micromosaic immunoassays (μMIAs), the analytes of interest were specifically captured with fluorescently labeled antibodies at the detection zone. The fluorescent signals revealed the specific binding in a single image step. With this method, the quantitative measurement of CRP was acquired for a small volume of human plasma (1 μL) within 10 minutes. This

combinational method for immunoassays could be applied to screen populations of patients with the coronary heart disease (CHD) and acute coronary syndromes (ACS). In another approach, an on-chip enzyme immunoassay of a cardiac marker, B-type natriuretic peptide (BNP), using a microfluidic device combined with a portable surface plasmon resonance system has developed by Kurita et al. [120]. They designed the T-shaped microfluidic channel for the purpose of flow-through solutions. The two patterned of gold thin film immunosensors were constructed (film A and B). Film A was embedded in the inlet port of microchannel, whereas film B was located downstream in the main microchannel. Before introducing the sample BNP solution into the channel, the BNP sample was interacted with the acetylcholine esterase-labeled antibody (anti- BNP−AChE). Then, a mixture solution was propelled from the inlet port to another inlet port. The unreacted anti-BNP−AChE was collected on BNP-modified film A during the first flow, and after that the channel was rinsed with phosphate buffer during the second flow. The acetylthiocholine was passed through the collected anti- BNP−AChE on the film A; therefore, thiocholine was produced. Finally, the thiocholine would be accumulated on the gold surface of film B and was monitored by the angle shift of SPR during the third flow. With this immunosensor approach, they could measure the BNP peptide with the detection range of 5 pg mL^{-1} - 100 ng mL^{-1} within 30 minutes.

Taking into account of cancer biomarkers, these makers can help to decrease the mortality rate due to the detection of disease at the early stage. More recently, there have been many significant biomarkers of cancer such as alpha-fetoprotein (AFP), prostate specific antigen (PSA), human carcinoembryonic antigen (CEA), and CA125. Thanks to the great specificity and sensitivity of antigen-antibody

interactions, the immunoassay is one of the most indispensable analytical techniques. Many previous works have reported on the approaches utilising microfluidic biosensor-based immunoassays for cancer diagnoses [121-124]. For example, Maeng et al. [122] have proposed a novel microfluidic biosensor based on an electrical detection system for alpha-fetoprotein determination. In their study, a sandwich immunoassay approach was applied to the system. The streptavidin coated microbeads were used to interact with biotinylated antibody and immuno-gold silver staining (IGSS) method was used to amplify electrical signals via platinum electrodes. Using this proposed configuration, the low limit of detection (1 ng mL^{-1}) was attained. Based on electrochemical detection, Panini et al. [123] has presented an immunoassay coupled to glassy carbon electrode (GCE) modified with multiwall carbon nanotubes (MWCNT) integrated with microfluidic system for PSA determination in serum samples. In another works, Sato et al. [121, 124] have demonstrated the integrated bead-based immunoassay in a microchip with using thermal lens microscope as a detertor. In their first approach, human secretory immunoglobulin A (s-IgA) was determined according to the interaction between the s-IgA coated on polystyrene beads and colloidal gold conjugated anti-s-IgA antibody [124]. The antigen-antibody complexes were detected by a thermal lens microscope. In later study, their proposed system was applied to determine the carcinoembryonic antigen (CEA) in serum samples [121]. Based on a sandwich immunoassay, a highly selective and sensitive determination of CEA was acquired within short analysis time.

As described above, there have been many practical applications of microfluidic device in real clinical analysis. Some of these works are listed in Table 7.

Table 7. Applications of microfluidic approach in clinical determination

Sample	Analytes	Microfluidic approach	Remarks	Ref.
Whole blood	Testosterone	PDMS chip with incorporation of membrane filter, RIA detection	On-chip sample preparation	[117]
Urine	Calcium	Quartz-PDMS microchip, reflectance measurement	Embedded ball lens for reflective mode	[22]
Serum	Calcium	Glass-PDMS microchip, reflectance measurement	Dye-immobilised on polymer beads	[26]
Urine	Albumin	PDMS-PDMS microchip, optical detection	Immunoturbidi-metric method	[24]
Urine	Creatinine	PDMS-PDMS microchip, optical detection	Alkaline picrate kinetic reaction	[25, 125]
Whole blood (spiked)	Sarin	PMMA microchip, fibre-optic detection	Integrated system with on-chip sample preparation and detection	[106]
Plasma (spiked)	C-reactive protein (CRP), myoglobin (Mb), cardiac Troponin I (cTnI), and protein S100α	PDMS microchip, fluorescent detection	Micromosaic immunoassays (μMIAs), sandwich format	[119]
Serum (spiked)	B-type natriuretic peptide (BNP)	Glass-PDMS microchip, immunosorbent assay, SPR detection	Competitive format, off-chip incubation	[120]
Serum	Alpha-fetoprotein (AFP)	PDMS-glass microchip with platinum (Pt) microelectrode, electric signal	Sandwich immunoassay	[122]

Sample	Analytes	Microfluidic approach	Remarks	Ref.
Serum (spiked)	Carcinoembryonic antigen (CEA)	Glass microchip for immunosorbent assay, thermal lens microscope	Sandwich immunoassay	[121]
Blood (spiked)	Hemoglobin	Silicon-glass microchip with two 45° mirrors, optical detection	Long optical path length (5 mm) with 45° mirrors	[107]
Serum	Prostate specific antigen (PSA)	Glassy carbon electrode modified with multiwall carbon nanotubes (CNT-GCE) integrated with microfluidic system, electrochemical detection	Electrochemical immunosensor	[123]
Saliva (spiked)	α-Thalassemia-1	Integrated system with three modules including gDNA extraction, PCR, and optical detection. fluorescent detection	Complicated system with PCR-based microfluidic device	[118]
Serum	Secretary human immunoglobulin A	Quartz-glass microchip, thermal lens microscope	Immunosorbent assay	[124]

CHAPTER III
MATERIALS AND METHODS

1. Chemicals and reagents

All chemicals were analytical reagent grade. Arsenazo III, bilirubin, and fluorescein sodium salt were purchased from Fluka (Buchs, Switzerland). 8-Hydroxyquinoline-5-sulfonic acid (8HQS), boric acid, haemoglobin, ascorbic acid, D-glucose, magnesium sulfate, and sodium chloride were obtained from Sigma (St. Louis, USA). Calcium carbonate was supplied by Mallinckrodt (USA). Iron standard, hydrochloric acid, and sodium hydroxide were acquired by Merck (Darmstadt, Germany). The calcium assay kit used for method validation was provided by Randox Laboratories (United Kingdom). The low (range 5.24-6.4 mg dL^{-1}) and high (range 11.2-13.6 mg dL^{-1}) levels of control serums (Liquid assayed multiqual®) from Bio-Rad Laboratories were intended for use as an assayed control serum to monitor the reproducibility studies. To get various amounts of analysts, the real serum samples were spiked with low or high levels of calcium from the commercial control serums before assaying. Poly(dimethylsiloxane) (PDMS, Sylgard 184) kits, for fabrication of PDMS microfluidic device, were provided from DowCorning (USA). Photoresist (SU-8 2100) and developing reagent were supplied by MicroChem (USA).

All solutions were prepared in Milli-Q water (Millipore, USA). Calcium stock standards (200 mg dL^{-1}) were prepared by dissolving 5 g of dried calcium carbonate in 1 M hydrochloric acid and diluting the solution to the desired volume of 1 L with Milli-Q water. Working calcium standards were freshly prepared by dilution of a stock solution in boric acid buffer before use. The 25 mM boric acid/sodium

hydroxide mixtures were used to maintain pH in the range of 8-9. Arsenazo III was used as specific dye binding throughout the experiment. The optimum concentration of arsenazo III was prepared in 25 mM boric acid buffer with 5 mM 8HQS, which is commonly used as a masking agent for the reagent.

2. Instruments

2.1 Instruments for fabrication of passive micromixer

The fabrication processes of micromixer were composed of mould fabrication, microchip fabrication, and surface treatment. In the mould fabrication process, a silicon wafer was used as the substrate. A photoresist material was spun on the silicon wafer by the spin coater (WS-400A-6NPP, Laurell technologies Corp., USA). The MJB4 mask aligner (SUSS microtec, Germany) was utilised as a machine in UV-photolithography technique to generate a master mould. To measure the height of embossed microstructure, the dektak profiler (Dektak 150, Veeco Inc., USA) was used as a mechanical device throughout the experiment. In the chip fabrication process, the vacuum pump (Harrick scientific Corp., USA) and the hot plate stirrer (Cole-Parmer Canada Inc., Canada) were employed. After completing the chip fabrication process, the PDMS surface treatment was carried out with the exposure to oxygen plasma. To bond the surface of PDMS-PDMS or PDMS-glass, the plasma cleaner (PDC-32G, Harrick Scientific Corp., USA) was used as a process of increasing the hydrophilic property.

2.2 Instruments for evaluation of mixing efficiency

The fluid mixing of two streams was observed by fluorescence microscope (BX10, Olympus, Japan) equipped with CCD camera (DP50, Olympus, Japan). To propel the two different fluids, the dual syringe pump (Fusion 200, Chemyx, USA) was employed.

2.3 Instruments for microfluidic system set-up

The microfluidic system for calcium determination included a dual syringe pump (Fusion 200, Chemyx, USA), two six-port injection valves (V-1461-DC and V-451, Upchurch Scientific, USA), in-house temperature controller, and miniature fibre optic spectrometer (USB4000, Ocean Optics Inc., USA). The single 600 µm UV-Vis fibre was used to transport light from the tungsten/halogen source (LS-1-LL, Ocean Optics Inc., USA) to the in-house flow cell, and the other 600 µm fibre connected to a USB4000 miniature spectrometer was horizontally positioned as a detector.

2.4 Instruments for calcium assay

The UV–Vis spectrophotometer (Evolution 600, Thermo Scientific, USA) was used as a reference method for comparison studies. The pH meter (Thermo Scientific, USA) was fully exploited to adjust the pH of boric acid/sodium hydroxide mixtures in range of 8, 8.5, and 9.

3. Experimental

3.1 Microfluidic simulation and design

3.1.1 Micromixer designs

The passive micromixer, a well-known device for mixing with a simple structure, has such advantages as simpler fabrication and easier integration with Lab-on-a-chip system**.** In a passive mixing, the design of the microchannels and obstructions is essential to raise the mixing performance [30, 33]. The optimal design of passive mixing system is necessary to study as a preprocessing step. In this study, a T-channel with four sets of ten J-shaped baffles placed in the microchannel was designed and simulated by using the multi-physics simulation software, COMSOL. The T-channel consisted of two inlet ports, which the two different fluids were dispersed to contact each other. Therefore, the complete mixing was expected downstream somewhere in the main microchannel. According to the schematic diagram (Fig.7), the main channel was 30 mm in length and the total length of four mixing sets was 25 mm. The width and depth of the main channel were 500 and 260 μm, respectively. For the J-shaped obstructions, all baffles were located at 70 and 150 μm from either side of the channel, respectively. The first J-shaped baffle was located at 900 μm as far away from the inlet. The distance between the adjacent J-shaped baffle was 170 μm and the space between each set of mixing region was 1,100 μm.

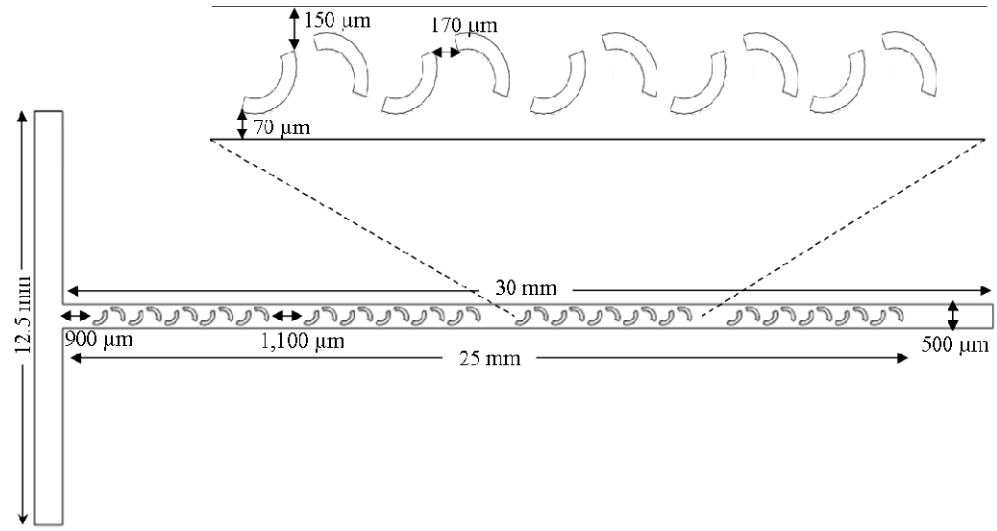

Figure 7. Schematic diagram of T-channel with four sets of ten J-shaped baffles in the main channel illustrates its dimensions; the microchannel was 500 µm wide and 260 µm high.

In order to investigate the effects of obstruction in T-type microchannel, two types of T-channel were modeled: with J-shaped baffles, and without J-shaped baffles. The mixing performance after passing through each set of ten J-shaped baffles was investigated by the simulation method.

3.1.2 Modeling method

The mixing efficiency was investigated using 3D simulations on COMSOL software to solve the conservation equations for mass, momentum, and diffusion-energy. Ethanol and water were introduced into two branches of a T-shaped microchannel. The simulation environment was verified for steady incompressible flows. The total number of cells in this micromixer was approximately 110,000 and the simulations were run for 250 iterations. To define the boundary conditions, the

three physical properties of the ethanol and water (density, viscosity, and diffusivity) were applied in the simulation as shown in Table 8. The no-slip condition was applied at the walls, and various flow velocities were subjected at the two inlets.

The mixing performance was investigated at five positions after passing through each mixing region. The quantitative analysis for mixing efficiency of mixer was based on the standard deviation of pixel intensity. At the chosen area, the standard deviation of the pixel intensity was determined across the channel width. A larger standard deviation indicates a lower mixing efficiency. The percentage of mixing efficiency was calculated by the equation described by Nguyen et al. [27].

Table 8. Properties of Ethanol and Water [83].

Fluid	Density (kg/ m^3)	Viscosity (kg/ms)	Diffusivity (m^2/s)
Water	9.998×10^2	0.9×10^{-3}	1.2×10^{-9}
Ethanol	7.890×10^2	1.2×10^{-3}	1.2×10^{-9}

3.2 Fabrication of passive micromixer and PDMS microfluidic device

The optimal design of passive mixing is clearly essential to raise the mixing performance in microfluidic channels. A passive micromixer can be easily generated by introducing the obstacles within channels or by modifying channel geometries [33, 86]. In this study, a T-channel with four sets of 10-piece, J-shaped baffles was designed using L-edit software. Each set of baffles was separated by a 1,100-μm long interval. The T-channel consisted of two inlet ports, where two different fluids were dispersed. The main channel was 25 mm long. The width and depth were 500 and 260

µm, respectively. The layout patterns were printed on transparencies, which were then used as a photomask in UV-photolithography to generate a master mould. A silicon wafer, which was utilised as the substrate, was subjected to piranha etching and dehydrated on a hot plate at 200°C. Afterwards, SU-8 2100, a photoresist material, was spun on the silicon wafer by a spin coater, as illustrated in Figure 8. Table 9 provides the details of spin speed, soft-baking time, post-baking time, and developing time for achieving the desired film thickness. After applying the photoresist to the substrate, it was soft baked to evaporate the solvent. Next, the photoresist-coated silicon wafer was exposed to UV light through a MJB4 mask aligner, as shown in Figure 9. The post-exposure, silicon wafer was post baked and then allowed to rest at room temperature overnight. The developing reagent was used to dissolve the unexposed regions and then the silicon wafer was rinsed briefly with isopropyl alcohol before being dried gently with a stream of air.

Table 9. The spin speed, soft-baking time, post-baking time, and developing time according to the manufacturer's instructions.

Product name	Viscosity (cSt)	Thickness (µm)	Spin Speed (rpm)	Soft-baking time (minutes)		Post-baking time (minutes)		Developing time (minutes)
SU-8 2100	45000	260	1000	65°C	95°C	65°C	95°C	20
				7	60	1	15	

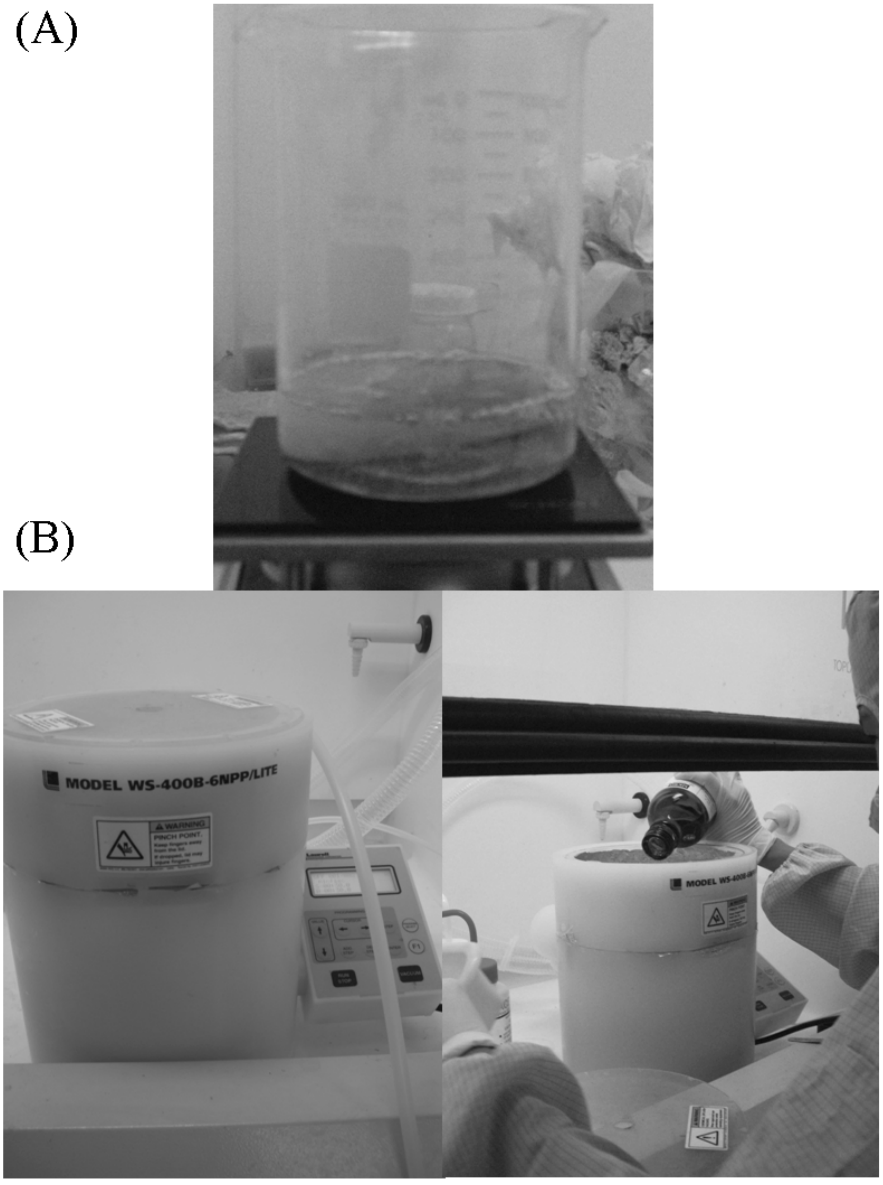

Figure 8. Photograph of the mould fabrication process according to the standard MEMS techniques illustrating (A) piranha etching (H_2SO_4 & H_2O_2) and (B) a photoresist material (SU-8 2100) spun on the silicon wafer.

(A)

(B)

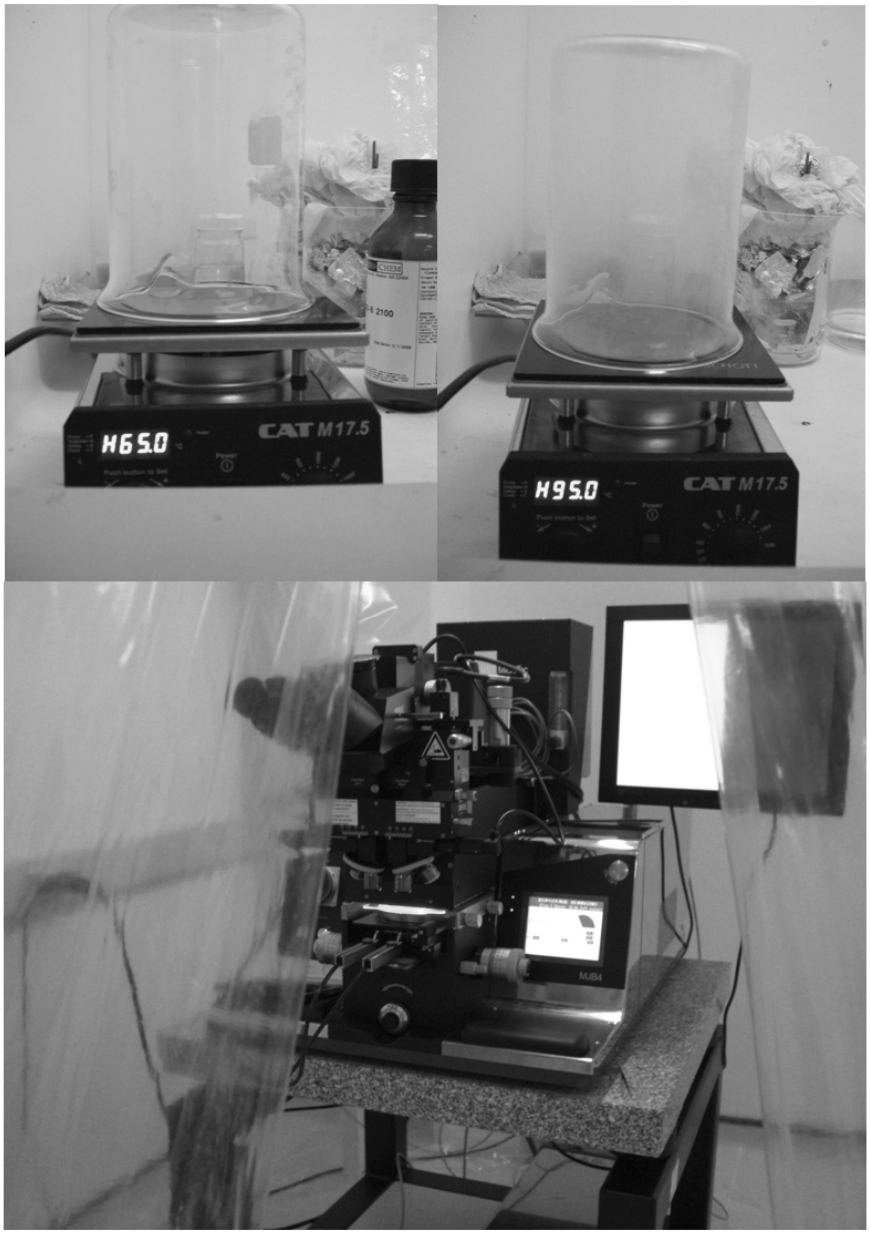

Figure 9. Photograph of UV-photolithography technique depicting (A) soft-baking and post-baking process at 65°C and 95°C, and (B) exposing to UV light through a MJB4 mask aligner.

After obtaining the desired silicon wafer through the mould fabrication process, the height of embossed microstructure was measured by dektak profiler. The Dektak 150 takes measurements electromechanically by moving a diamond-tipped stylus over the sample surface, as shown in Figure 10.

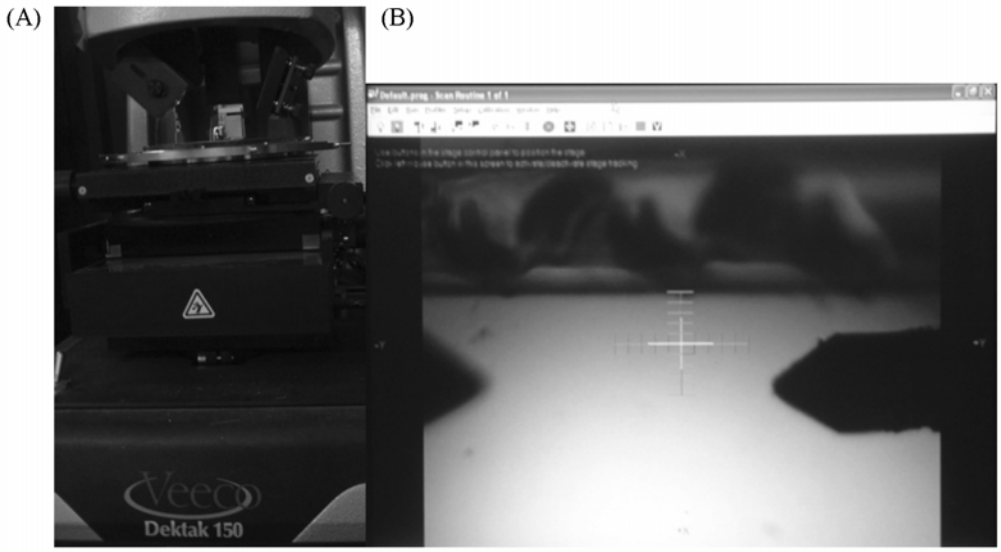

Figure 10. Photograph of Dektak 150 showing (A) the measurement of physical silicon surface by a diamond-tipped stylus, and (B) a programmable positioning system controlling the stylus on the sample.

In this research, two types of chips were fabricated: (i) a PDMS-glass and (ii) a PDMS-PDMS layered chip. The microchip, which was applied to evaluate the mixing performance and was observed under a fluorescence microscope, was fabricated using PDMS-glass layering. The micropattern of PDMS was generated on an embossed microstructure by a replica moulding method. The PDMS base and

curing agent were mixed well (10:1, w/w) and degassed before pouring onto the design structure of the silicon wafer. Next, the PDMS was cured at 70°C for 1 hour and then peeled off. Small holes were drilled into the PDMS using a borer to produce two inlets and an outlet. Finally, the replica PDMS was sealed to the glass slide by oxygen plasma using a plasma cleaner (PDC-32G, Harrick Scientific Corp., USA). After completing the surface treatment process, Tygon tubing (Bio-Rad Laboratories, USA) was connected to the fabricated microchip to provide two inlets and an outlet.

A microfluidic chip used for determining calcium levels was fabricated based on PDMS-PDMS bonding, as depicted in Figure 11. This platform consisted of an upper and lower PDMS layer. The upper PDMS layer was cast from the J-shaped structure of the silicon mould, and holes were punched for two sample inlets and then the lower PDMS layer was sealed. To construct the lower PDMS layer, a mixed pre-polymer was spread over a flat master mould and heated at 70^{o}C. After curing, a 60 µL in-house flow cell was placed on the PDMS surface. Next, additional polymer was poured over the flat PDMS layer, and finally, the embedded flow cell PDMS layer was peeled off from the flat master mould. A hole was punched at the top of the flow cell to collect the mixture of fluids. Both the upper and lower PDMS layers were then treated with oxygen plasma and immediately bonded together. Afterwards, Tygon tubing was connected to the PDMS microfluidic device to provide two sample inlets. A similar microchip fabrication incorporating an in-house flow cell into a PDMS-PDMS microchip has been previously reported by our group [24-25].

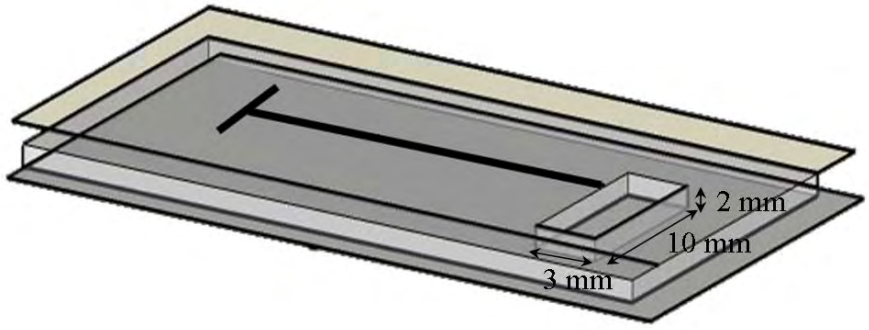

Figure 11. Schematic diagram of PDMS-PDMS microfluidic device for calcium assay: the upper PDMS layer and the embedded flow cell PDMS layer.

3.3 Evaluation of mixing efficiency

Mixing efficiency of the micromixer was evaluated based on the captured fluorescence images. One syringe was filled with a solution of 100 µM fluorescein in Milli-Q water (subjected to the inlet), and another syringe was filled with Milli-Q water. The two syringes were injected at various flow rates ranging from 10 µL min^{-1} to 100 µL min^{-1}, using a dual-syringe pump. The mixing of two streams was observed under a fluorescence microscope (BX10, Olympus, Japan) equipped with a CCD camera (DP50, Olympus, Japan). The system setup for evaluation of mixing efficiency is shown in Figure 12. The mixing performance was observed at five positions after passing through each set of J-shaped baffles. The captured images were converted into grey scale before determining the standard deviation of a chosen cross-

channel width (5 x 450 pixels area). In this study, the standard deviation (C) of the fluorescent intensity at each area was determined by the equation defined by Nguyen et al. [27]:

$$C = \sqrt{\frac{1}{N}\sum_{i=1}^{N}(I_i - I_{mean})^2}$$

where N is the number of pixels, I_i is the intensity at pixel I, and I_{mean} is the mean intensity of all regions, respectively. Commonly, a larger standard deviation indicates a lower mixing efficiency. The percentage of mixing efficiency (C_{mix}) was calculated using the following:

$$C_{mix} = \frac{C_{inlet} - C}{C_{inlet}}$$

where C and C_{inlet} represent the standard deviations of the chosen area and of the inlet, respectively [27].

To verify the results acquired from the fluorescence image acquisitions, it had to be assured that the mixing results would be identical to those of the computational simulation.

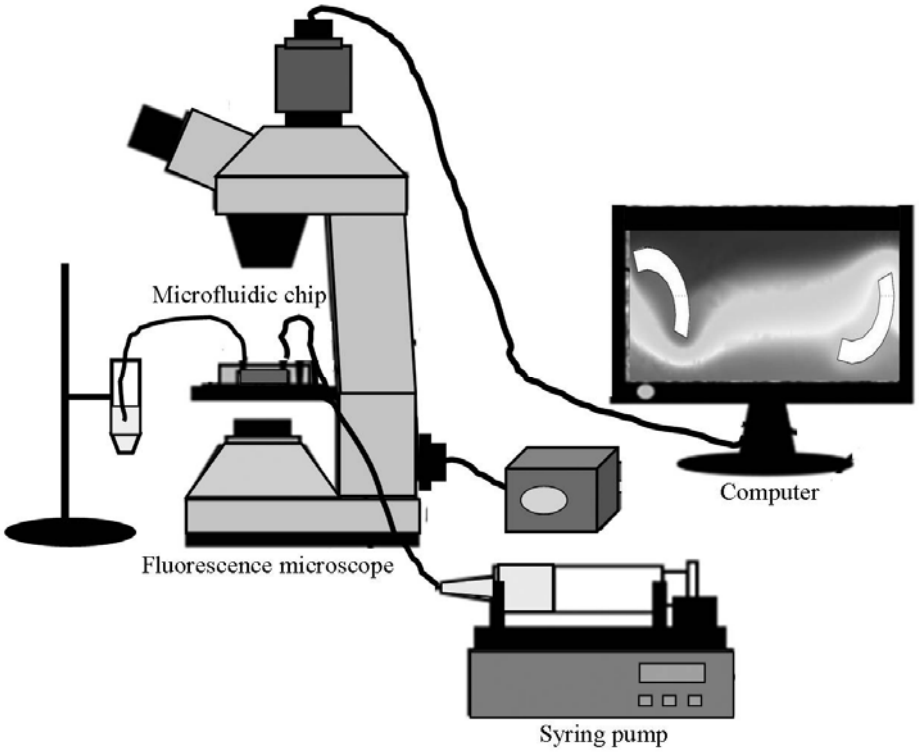

Figure 12. Experimental fluorescence set-up for charcterising micromixer performance (Modified from [126]).

3.4 Microfluidic system set-up

The microfluidic system for calcium level determination included a dual syringe pump (Fusion 200, Chemyx, USA), two six-port injection valves (Upchurch Scientific, USA), a microfluidic micromixer chip, an in-house temperature controller, and a miniature fibre optic spectrometer (USB4000, Ocean Optics Inc., USA), as shown in Figure 13. The dual syringe pump supplied carrier buffer via plastic syringes (Terumo Co., Japan), whereas the two six-port injection valves were separately used to load the sample and arsenazo III reagent. The absorbance increments, resulting from the chemical reaction, were measured via the fibre optic spectrometer at 650 nm.

A single 600 µm UV-Vis fibre transported light from the tungsten/halogen source (LS-1-LL, Ocean Optics Inc., USA) to the in-house flow cell, while another 600 µm fibre connected the USB4000 miniature spectrometer that was horizontally positioned as a detector. In addition, the calcium-arsenazo III complexes were determined at a constant temperature, due to the temperature controller regulating the experiment.

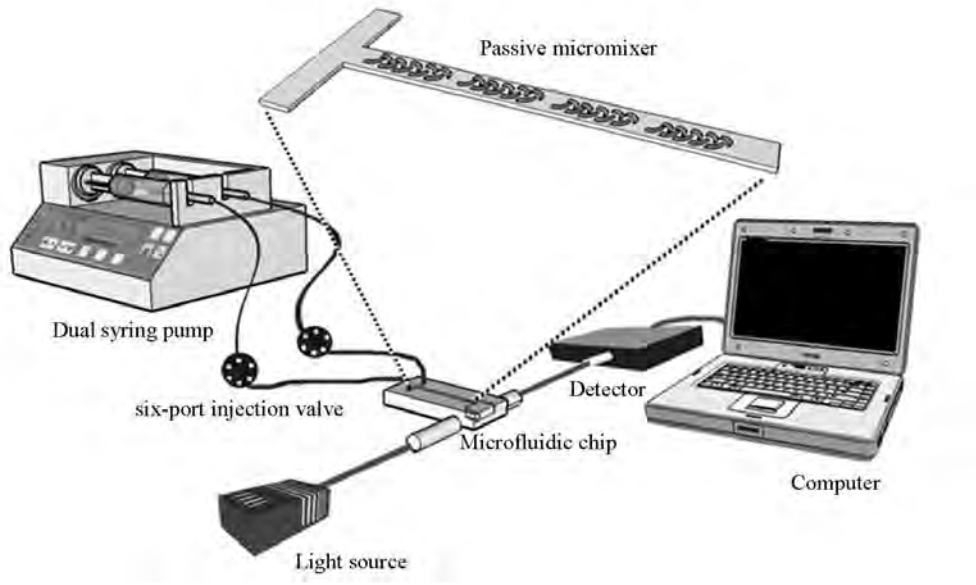

Figure 13. Configuration of the microfluidic system and detailed view of the passive micromixer with J-shaped baffles [127].

3.5 Microfluidic system for calcium assay

In this proposed system, calcium was quantitatively assayed with a specific dye binding method utilising arsenazo III. When the dye reacted with calcium to form a blue-purple coloured complex, the reaction was quantified by an embedded

miniature fibre optic spectrometer monitoring absorbance increments at 650 nm. The intensity of the colour was proportional to the calcium concentration.

The dual syringe pump delivered 25 mM boric acid carrier buffer via plastic syringes, at a constant flow rate of 40 µL min^{-1}. The injection valve was utilised to subject the 2-µL serum samples to the system, while a separate valve was used to load the 25-µL arsenazo III reagent. Before the analysis of calcium, a solution of 1 M hydrochloric acid was flowed onto the microchip and subsequently washed with the carrier buffer. The acid wash step is included in this calcium assay procedure to remove trace contaminations of the calcium ion from the system. When the serum sample and arsenazo III were dispersed together at the inlet of the microchip, a homogeneous mixture was expected downstream after passing each set of 10 J-shaped baffles. The calcium-arsenazo III complexes generated their full colour intensity at the detection zone. After finishing each injection process, the regeneration of the chip was performed by introducing 1 M hydrochloric acid (HCl) solution and subsequently washing with a carrier buffer. This step was repeated until the absorbance signal returned to the original baseline.

3.5.1 Assay optimisation

The performance of proposed system was considered in detail as listed below:

- Ratio of sample/reagent

For the current large scale method, approximately 1000 µL of arsenazo III reagent was utilised for each calcium assay. Using this approach, the enormous amount of reagent can cause the environmental pollution. The main aim of this work

is to reduce the arsenic toxicity; thus, the sample-to-reagent ratio was optimised for receiving the appropriate signal response.

- Absorbance spectra of calcium-arsenazo III complex

By using an Ocean Optics USB4000 miniature fibre-optic spectrometer, the calcium-arsenazo III complex was observed under the spectra of visible wavelengths at 400-800 nm. The wavelength providing the highest peak of absorbance was selected for the subsequent experiments.

- Reaction time

After stopping the dual syringe pump, the absorbance signals of dye binding formation were recorded for 3 minutes. In order to select the optimal time for calcium assay, the rate of colour development was investigated until the chemical reaction rate was constant.

- pH of carrier buffer

The effect of pH on absorbance measurement was investigated because the formation of calcium-arsenazo III complexe occurs in a wide pH range. In this study, the boric acid/sodium hydroxide solutions were selected to maintain the pH in the range of 8, 8.5, and 9.

- Concentration of arsenazo III reagent

The reagent concentration is an important parameter that can affect the sensitivity of calcium assay. Hence, the arsenazo III concentration was investigated in the range of 200-500 μM.

- Temperature

Using the in-house temperature controller, the investigation of temperature effect was carried out at 25, 30, 35 and 37°C.

3.5.2 Assay characterisation

The proposed system was characterised as an efficient method, including the following:

- Linearity

Under the proper condition, the proportional relationship between the concentration of calcium and the analytical signal was plotted to produce an analytical curve.

- Sensitivity (limit of detection)

Sensitivity means the ability of the method to detect an analyte, whereas the limit of detection (LOD) is the lowest concentration level that can be determined to be different from the blank. The reagent blank was analysed for 10 times, and then the response signals were calculated the standard deviation. The LOD was assessed as 3 times of standard deviation divided by the slope of the calibration curve.

- Precision (Reproducibility)

Precision is sometimes referred to reproducibility, which is a measure of the repeated measurements of each sample. Precision is determined by the coefficient of variation, which is defined as the standard deviation divided by the average of replicates. Two levels of control serum were assayed for calcium content to study the reproducibility of the proposed system. Within-run reproducibility was performed with low- and high-level control serums on the same day (each concentrations n = 10). In addition, run-to-run reproducibility was assessed by assaying low- and high-level control serums on three different days (n =30).

- Carry-over effect

Carry-over is commonly used to describe a process by which the reagents or samples are transferred into another reaction. The carry-over effect between consecutive samples was determined by analysing a sample in duplicate with a high analyte concentration and following in triplicate by a low analyte concentration. The carry-over effect was then calculated using the following formula [128]:

$$\text{Percentage of carry-over effect} = \frac{(b1-b3)}{(a2-b3)} \times 100$$

where a1, a2 are the high analyte concentration, and b1, b2, b3 are the low analyte concentration, respectively.

- Specificity (Interferences)

It is necessary to ensure that the other substances could not affect the performance of calcium assay. For this reason, the interference study was carried out. The various substances were investigated, i.e. sodium, magnesium, iron, glucose, ascorbic acid, haemoglobin, and bilirubin. A known amount of interference was spiked into the control serum samples, and then the percentage recovery was calculated from the ratio of the initial response signals to the spiked signals.

- Assay comparison

Fifteen students from Faculty of Allied Health Sciences at the age of 20-30 were invited to participate in this research project. Every volunteer who takes part in this study has to be well-informed and participate of his or her own volition. All the participants should fast at least 6 hours before venipuncture. Serum samples from these healthy volunteers, including low and high spiked calcium serums (n = 15), were assayed via this proposed method. The obtained results were validated with those of a conventional spectrophotometer using a commercial calcium kit from Randox Laboratories. A 650-nm detection wavelength was used according to the manufacturer’s instructions for the UV-VIS spectrophotometer.

CHAPTER IV
RESULTS

1. Micromixer design and its mixing performance

1.1 Numerical simulations

In order to investigate the mixing performance of the proposed micromixer, the multi-physics simulation software, COMSOL, was used for the computational analysis. The simulation environment was verified for steady incompressible flows of the test fluids, i.e. ethanol and water. To investigate the effect of obstructions, two types of T-channel were modeled, including the plain T-type micromixer, and T-type micromixer with J-shaped baffles in the main channel. The mixing performance of two different fluids was investigated at five locations. At each position, the quantitative analysis of mixing efficiency was related to the standard deviation of pixel intensity across the channel width. The percentage of mixing was calculated by the equation described in Chapter 3.

The simulation results of two different designs of micromixer were compared at the flow rate of 40 μL min^{-1}, as shown in Figure 14. The results indicated that the T-type micromixer can only reach around 60% mixing performance, whereas the T-type micromixer with four sets of J-shaped baffles in the main channel can be achieved almost 90% mixing performance at the end of channel. Within a total length of 30 mm of micromixer, it was supposed that this J-shaped micromixer could achieve 100% mixing performance at the end of channel.

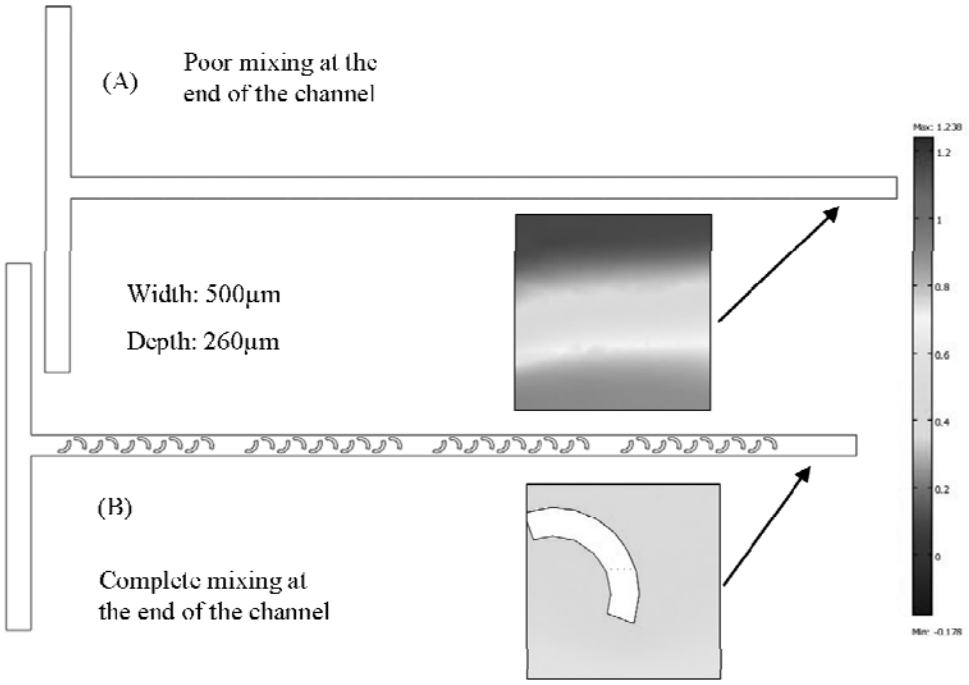

Figure 14. Comparison of micromixer designs; (A) plain T-type micromixer and (B) T-type micromixer with four sets of J-shaped baffles in the main channel.

The performance of the proposed design (Fig.14) implied that the J-shaped obstacles could enhance the mixing of the two fluids by introducing the lateral convection in the main channel. After passing four sets of mixing region, the homogeneous mixing almost completed. Baffles within the microchannel can encourage chaotic flow of the fluid. As shown in Figure 15, the concentration distributions of ethanol gradually became homogeneous as the downstream mixing-sets increased. The streams of concentration changed into uniform mixing after passing two sets of J-shaped baffles. The flow velocity profile was depicted in Figure 16, the results demonstrated that the velocity near the microchannel sidewalls is lower than that at the center. The mixing near the J-shaped baffles can lead to the lateral perturbation; therefore, it enhanced the mixing of two different fluids.

Figure 15. Concentration distributions of ethanol from the simulation results at the flow rate of 40 μL min^{-1}.

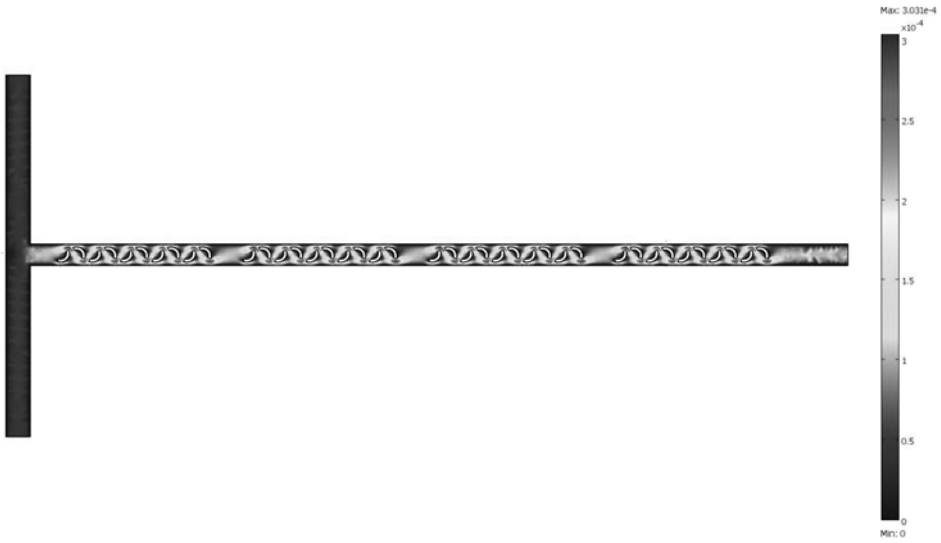

Figure 16. The flow velocity profile of T-type microchannel with four sets of ten J-shaped baffles at the flow rate of 40 μL min^{-1}.

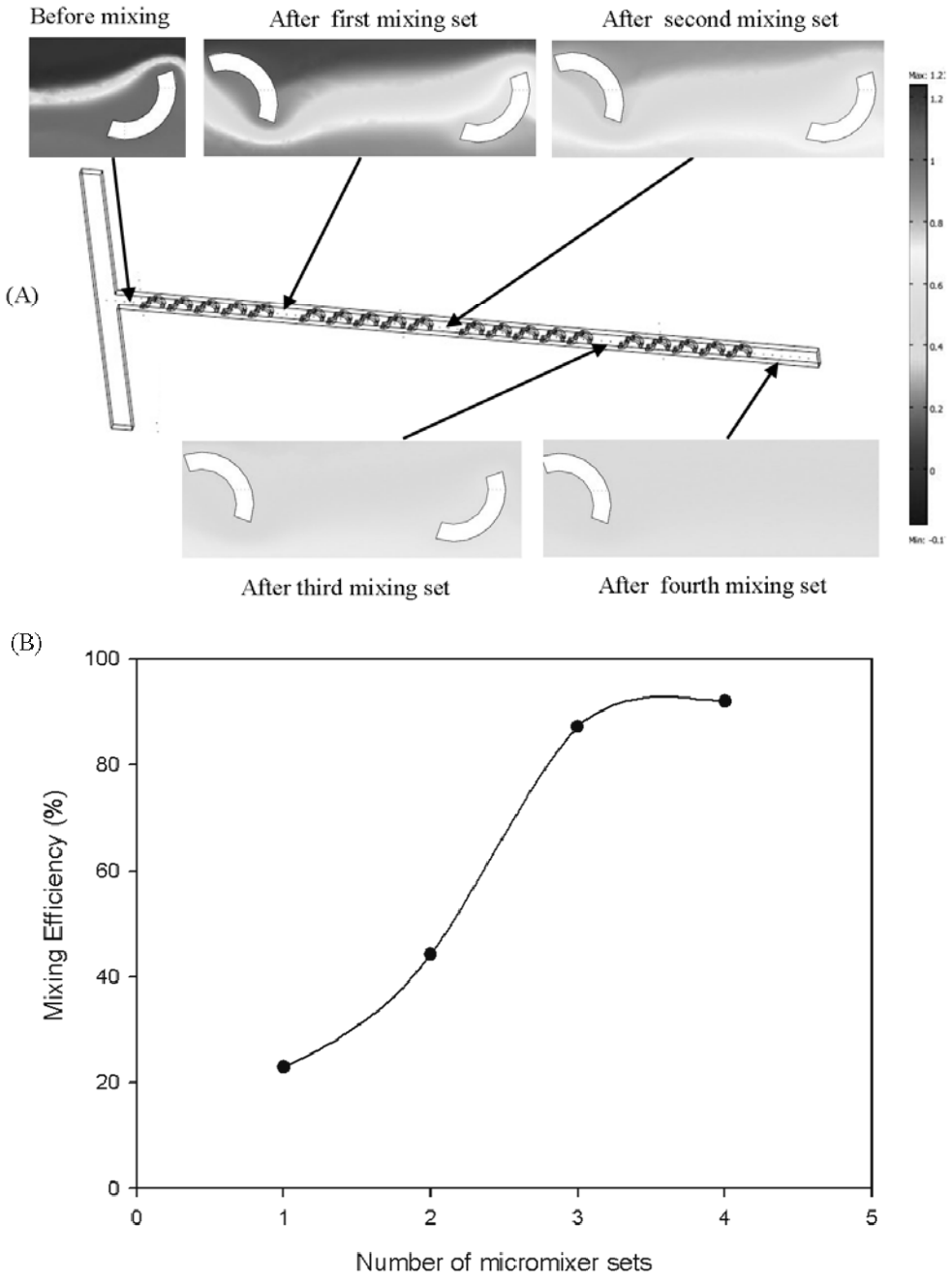

Figure 17. Schematic diagram of four mixing regions, which each one was composed of ten J-shaped baffles in the main channel: (A) The close-up of concentration distributions of ethanol from the simulated results; (B) Simulation results of mixing efficiency after passing each mixing region at the flow rate of 40 μL min^{-1}.

According to the simulation, it was clearly indicated that almost complete mixing was achieved after the solution passed through four mixing sets of J-shaped baffles; in other words, its contents became gradually homogeneous, as shown in Figure 17(A). In Figure 17(B), the standard deviation of the pixel intensity distribution was measured in the images of the cross-section of the channel at varying distances from the entrance. The proposed micromixer was achieved almost 90% mixing performance after passing four mixing sets. These computational simulation results illustrated that the proposed micromixer was a valuable model for integration into Lab-on-a-chip system.

1.2 Mould fabrication process

It is necessary to ensure that all of the J-shaped obstructions were approximately equal in height. Hence, the desired silicon wafer was measured by using dektak profiler. The height of main microchannel was observed at five positions after passing through each set of J-shaped baffles. As shown in Figure 18, the results indicated that the channel height of all the five positions were maintained the optimum levels of 260 μm.

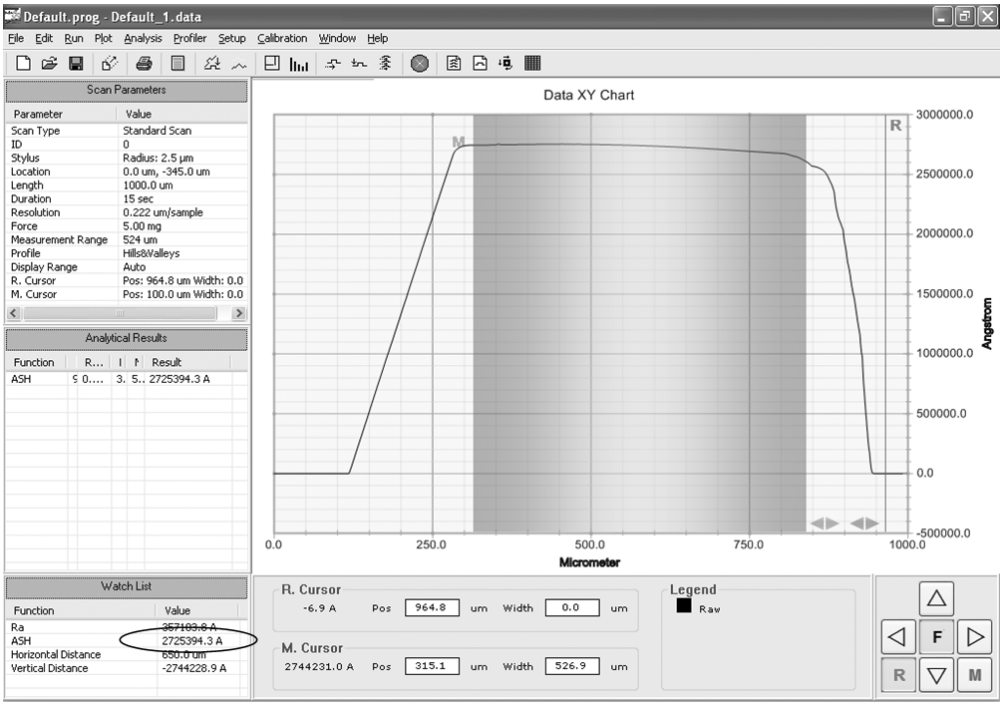

Figure 18. A programmable surface measuring system illustrates the surface analysis software for calculating the height of the embossed microstructure.

1.3 Fluorescence set-up for evaluation of mixing efficiency

Although a similar microchip-based system has been implemented in our group [24-25], the fluorescence experiment to exam the mixing capability had yet to be investigated. To verify the results acquired from the fluorescence image acquisitions, it had to be assured that the mixing results would be identical to those of the computational simulation. If those could be affirmed, our proposed microfluidic chip would pose to be a valuable model for clinical analysis. The passive microfluidic mixer with J-shaped baffles in the T-channel was first put forward by Lin et al. [129]. They asserted that their design was particularly suitable for on-chip blood analysis. However, the application for on-chip biochemical analysis was not yet fully exploited.

Therefore, the T-channel with a modified J-shaped structure was employed for our mixing purpose.

The fluorescence technique was used to evaluate the mixing efficiency in the microchannel. As mentioned earlier, the experimental set-up for mixing characterisation consisted of a fluorescence microscope equipped with CCD camera, a dual-syringe pump and a microfluidic device. The solution of 100 μM fluorescein and DI water were introduced into the two inlets with the flow rate of 40 μL min^{-1}. The mixing of two streams was observed under the fluorescence microscope and the mixing efficiency of the micromixer was evaluated based on the captured fluorescence images. The images were captured at five positions, and then were converted into grayscale before evaluating the standard deviation of a chosen area across the channel width (5 x 450 pixels area). In this study, the standard deviation (C) of the fluorescent intensity at each area was determined by the equation described by Nguyen et al. [27]. Figure 19 illustrates the gray-scale line scans of fluorescent intensity across the channel width at the inlet and outlet. According to Figure 19(A), the fluorescein solution was introduced into the upper section of the captured image and DI water into the lower section. Thus, the downward trend in fluorescent intensity was expected to start from the upper to lower section. Meanwhile, the captured image at the outlet had equivalent in fluorescent intensity across the channel width, as shown in Figure 19(B).

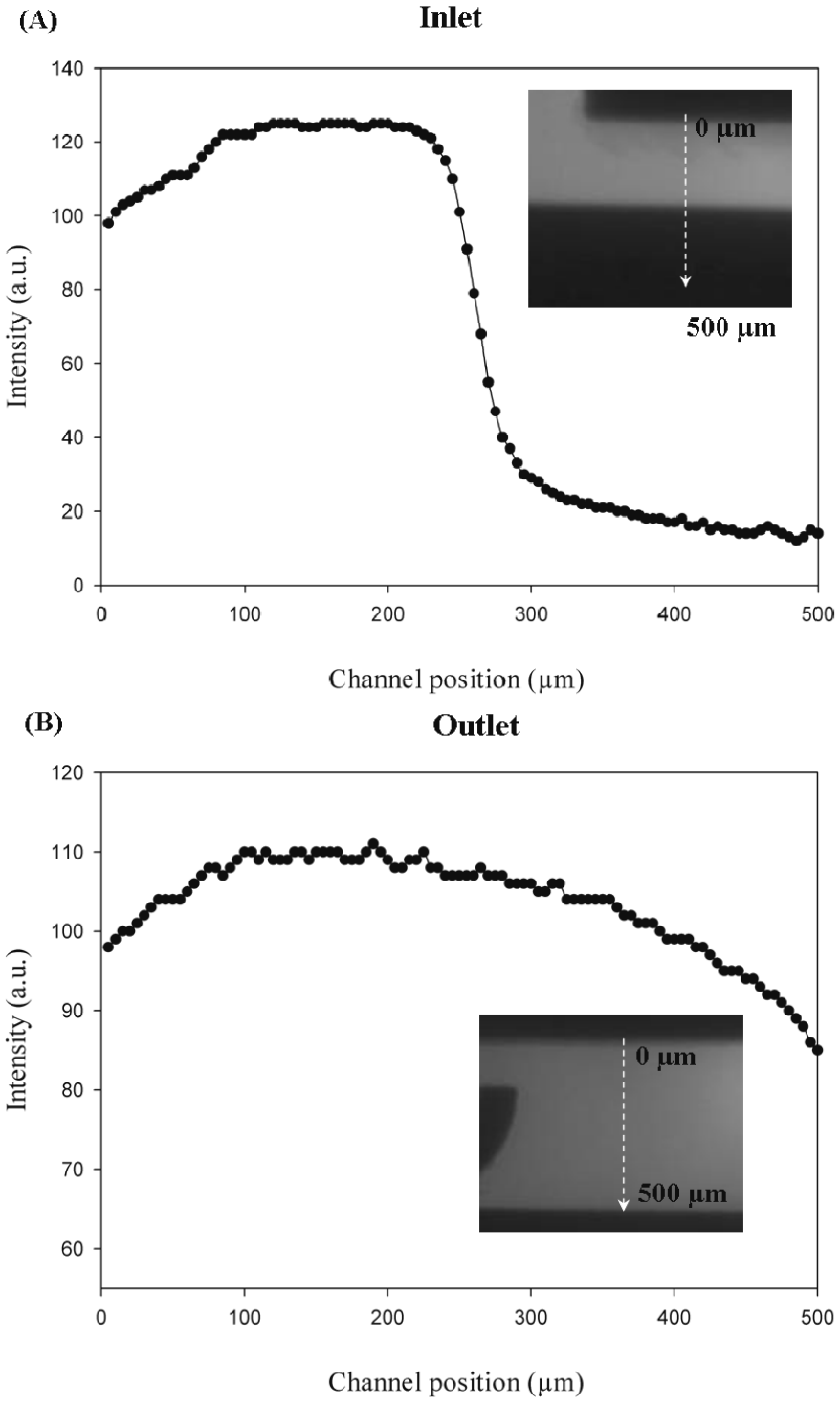

Figure 19. The cross-section line scans of fluorescent intensity across the channel width indicating the mixing of two fluids at (A) the inlet and (B) outlet.

Both T-type micromixer and T-type micromixer with four sets of J-shaped baffles within the main channel were characterised for their mixing performance by utilising our fluorescence set-up system. Compared to their percentage of mixing capability, the results indicated that the proposed design could improve the quality of its mixing. As shown in Figure 20, the T-type micromixer is achieved almost 50% mixing performance. By contrast, the proposed design is obtained around 85% mixing performance at the end of channel.

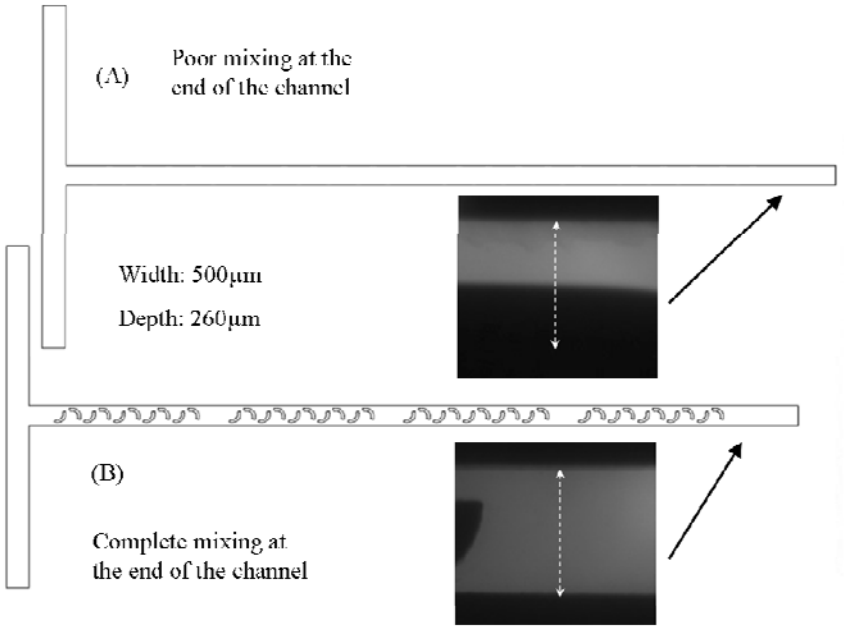

Figure 20. Comparison of two fluorescent captured images; (A) T-type micromixer and (B) T-type micromixer with four sets of J-shaped baffles in the main channel.

According to the captured fluorescent imaging results (Fig.21A), the homogeneous mixing was achieved after passing four mixing sets of J-shaped baffles. In Figure 21(B), the mixing efficiency was calculated at varying distances from the entrance. The proposed micromixer was achieved almost 85% mixing performance after passing four mixing sets.

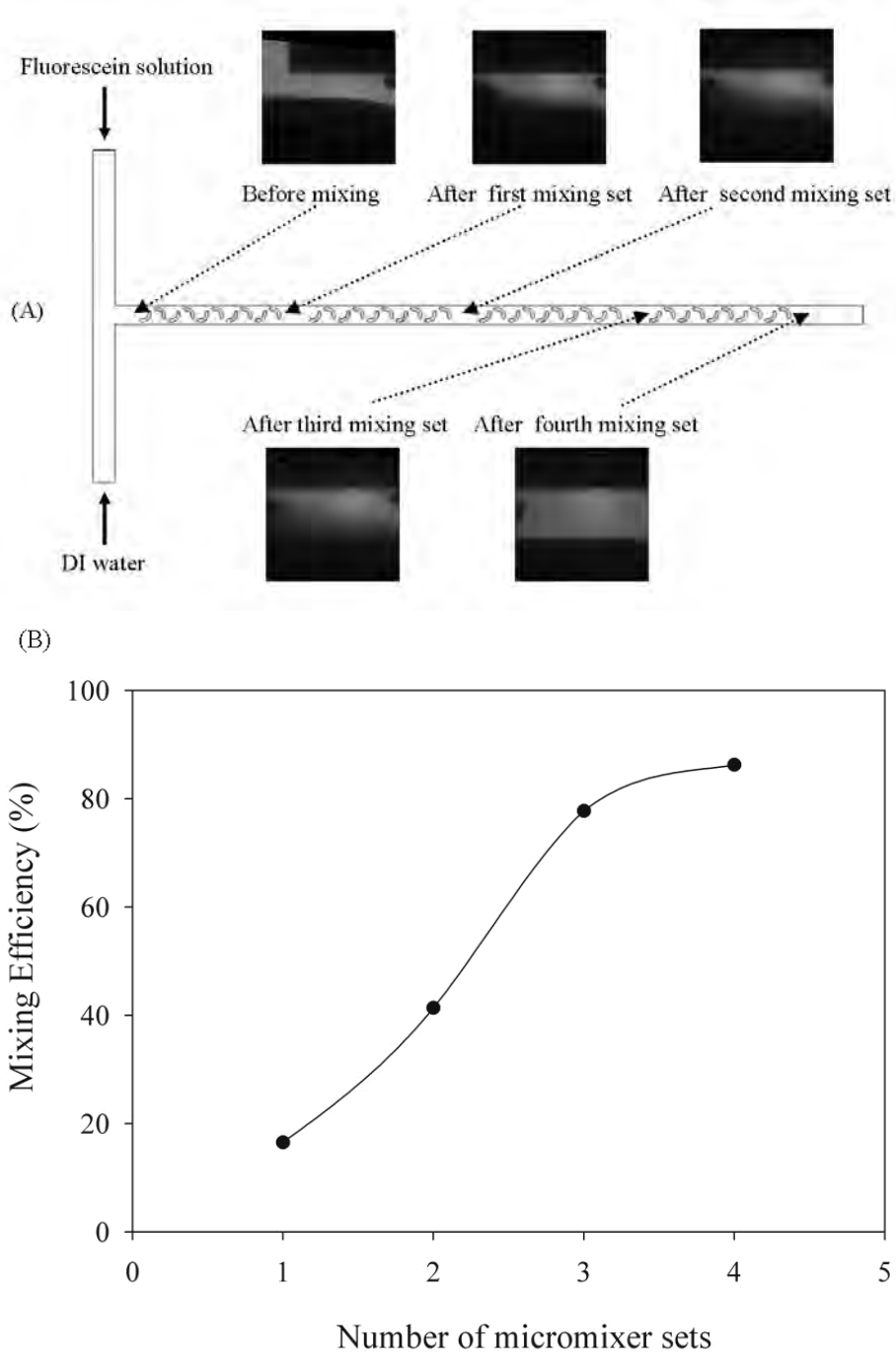

Figure 21. Experimental results illustrating the charactersation of mixing performance: (A) The solution of 100 μM fluorescein was injected into the upper section and DI water into the lower section; (B) Evaluation of mixing efficiency after passing each mixing set at the flow rate of 40 μL min^{-1}.

1.4 Comparison between simulation and fluorescence characterisation

As shown in Figure 22, the mixing percentage between the simulation and the fluorescence results are represented. Our proposed design enhanced the mixing of the two fluids by introducing lateral convection in the microfluidic channel. In addition, baffles within the microchannel strongly encouraged chaotic flow. As a result, the fluid distributions gradually became homogeneous as the downstream mixing-sets increased. Additionally, a homogeneous mixing was attained in a short time and within a limited length; a mixing percentage of ~90% homogeneity was obtained after passing all mixing regions, which accounted for a 25-mm length. Therefore, considering the total length of the microchip, ending at the detection zone, was 30 mm, it was assumed that a complete mix could be accomplished. Unfortunately, while the mixing tendency was similar in both curves, the percentage of mixing with the real fluorescence experiment was 5% lower than that of the simulation results. This lower mixing efficiency might be due to the surface roughness factor in the simulation and the error in fabrication process. However, it could be concluded that this proposed micromixer could incorporate into the microfluidic system and enhance the mixing performance of two different fluids.

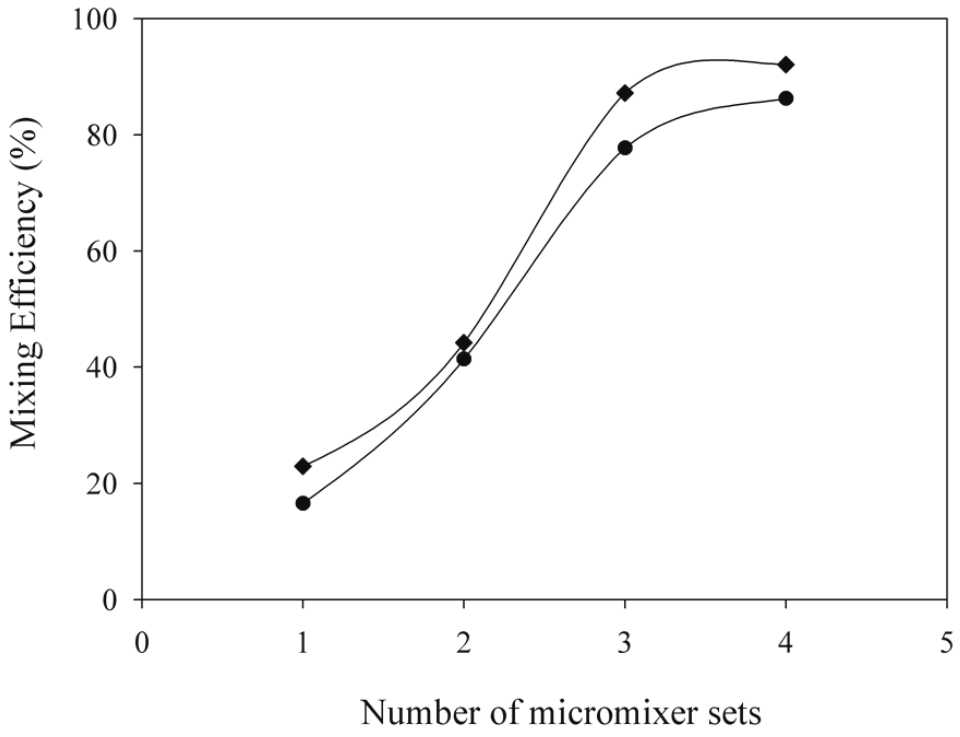

Figure 22. Comparison between the mixing percentage of simulation results (♦) and that of experimental results (●) [127].

The mixing performances at flow rates of 5, 10, 20, 40, 60, 80, and 100 µL min^{-1} were also investigated by using fluorescence technique, as shown in Figure 23. The results implied that this proposed micromixer was achieved almost 90% mixing efficiency over the wide range of flow rates. When the flow rate was over than 40 µL min^{-1}, the microfluidic devices always faced the problem of device leakage. Hence, the flow rate of 40 µL min^{-1} was selected as a compromise between mixing efficiency and pressure driven-force for all subsequent experiments.

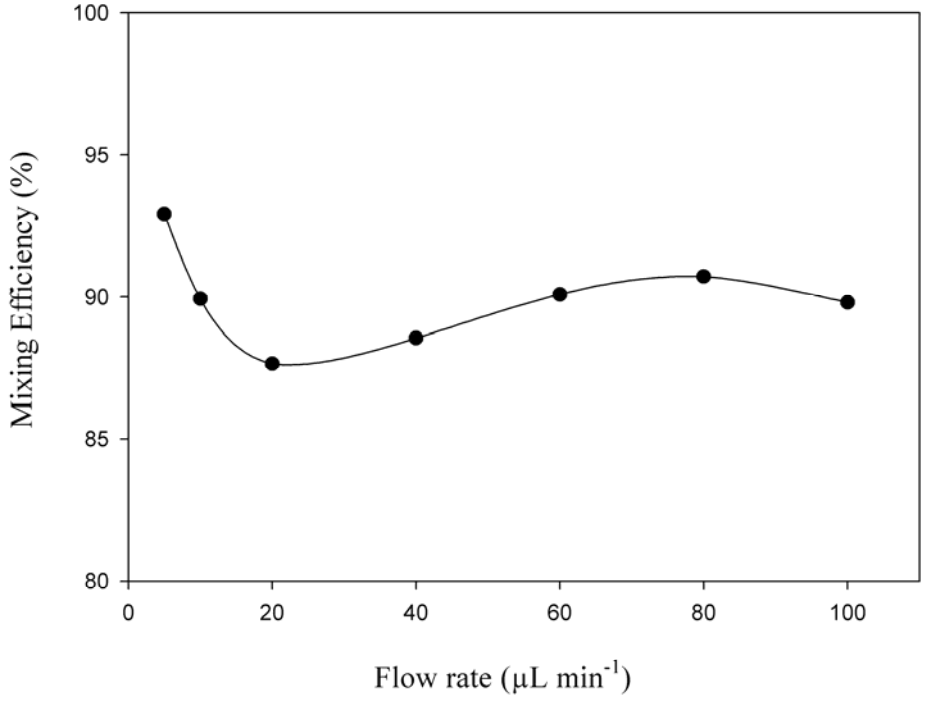

Figure 23. A mixing examination of fluorescence characterisation at different flow rates: 5, 10, 20, 40, 60, 80, and 100 μL min^{-1}.

2. Calcium assay optimisation

2.1 Spectrum of calcium-arsenazo III complex

After completing in reagent preparation for calcium determination, all the reagent solutions were tested for their quality before they were assayed in microfluidic system. Initially, a conventional UV–Vis spectrophotometer was used as a method of choice to examine the chemical characteristics of reagents. As shown in Figure 24, the absorbance spectrum was observed under the condition of 400 µM arsenazo III in 25 mM boric acid buffer combined with 5 mM 8HQS. The calcium concentration of 3 mg dL^{-1} was assayed at a pH of 8. The shape of spectrum appeared to reach a maximum absorbance at the wavelength of 650 nm. As a result, the peak absorbance at 650 nm was selected for all subsequent experiments.

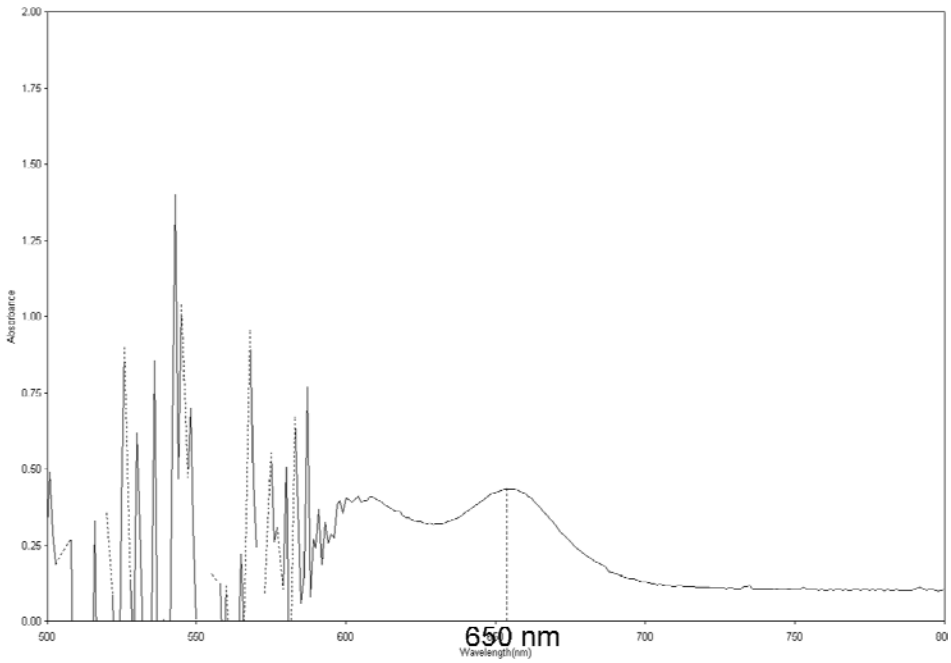

Figure 24. Spectrum of calcium-arsenazo III complex in the reagent containing 5 mM 8HQS.

2.2 Optimum ratio of sample-to-reagent

This work aims to implement a greener analytical method for calcium assaying by diminishing the consumption of the arsenazo III reagent. In other words, the appropriate ratio between the sample and the arsenazo III reagent needs to be optimised. Current large-scale methods for the determination of calcium levels require the sample-to-reagent ratio to be 1:100, which requires an enormous amount of reagent. Based on a conventional spectrophotometric method, approximately 1,000 µL of arsenazo III reagent is used in each assay. In this work, we have designed an in-house flow cell using a total volume of 60 µL, which significantly decreases the total reagent consumption by about 15 fold. The arsenazo III reagent was tested at various volumes of 25, 50 and 75 µL, where the sample volumes were fixed to 2 µL. Calcium concentrations of 0.2 and 3 mg dL^{-1} were assayed in duplicate for three different ratios. As shown in Figure 25, the results demonstrated that the pattern of response signals of 0.2 and 3 mg dL^{-1} of calcium were quite similar for all three different ratios; subsequently, increasing the reagent volume did not improve the sensitivity of the assay. When the arsenazo III reagent volume was increased to 75 µL, the signal response remained exactly equal to those obtained for 25 µL and 50 µL. As a result, a ratio of 2:25 µL was selected for subsequent experiments. Besides the clean analytical benefit, using less arsenazo III reagent can also shorten both the reaction and regeneration times.

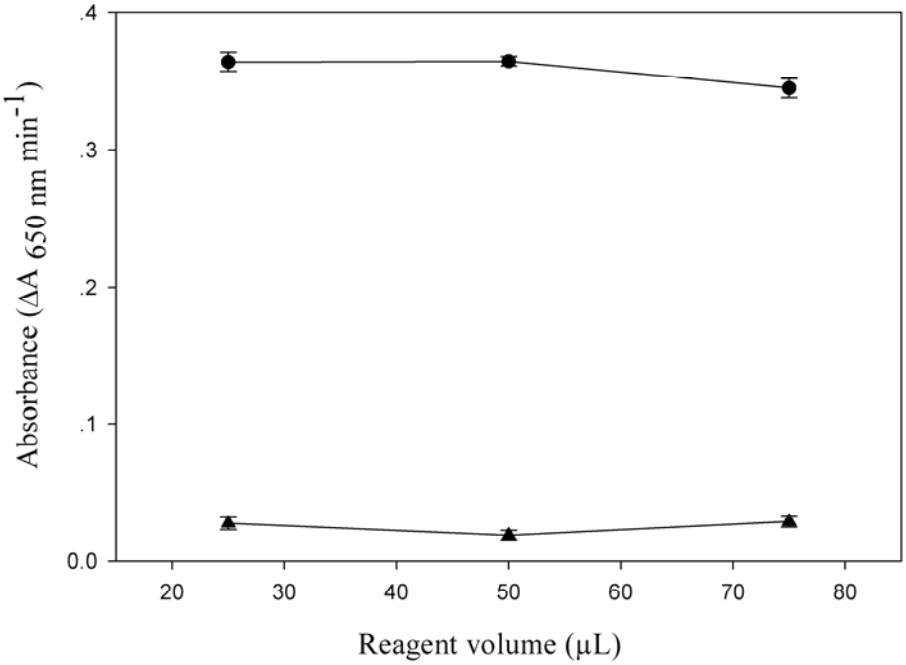

Figure 25. The effect of increasing arsenazo III reagent volume on absorbance sensitivity (▲) 0.2 mg dL^{-1} calcium; (●) 3 mg dL^{-1} calcium.

2.3 Reaction time optimisation

Owing to the change in sample-to-reagent ratio, the reaction time was under investigation for the best response signal. Unless otherwise stated, the injection valve was utilised to subject the 2-µL calcium samples to the system, while a separate valve was used to load the 25-µL arsenazo III reagent. The calcium concentration of 3 mg dL^{-1} was assayed in duplicate for monitoring the reaction time. When the arsenazo III reagent reacts with calcium to form a purple-coloured complex, the increment of absorbance was measured at the wavelength of 650 nm. The absorbance signal of dye binding formation was recorded after stopping a dual-syringe pump for 3 minutes. According to calcium-arsenazo III reaction (Fig.26), the results implied that the

optimal time for calcium assay was 1 minute. Since the linear response was gained within a minute, the collection of absorbance signal was recorded during this period of time. Indeed, this proposed system demonstrated the improvement on short reaction time of calcium assay because the test around time was significantly reduced.

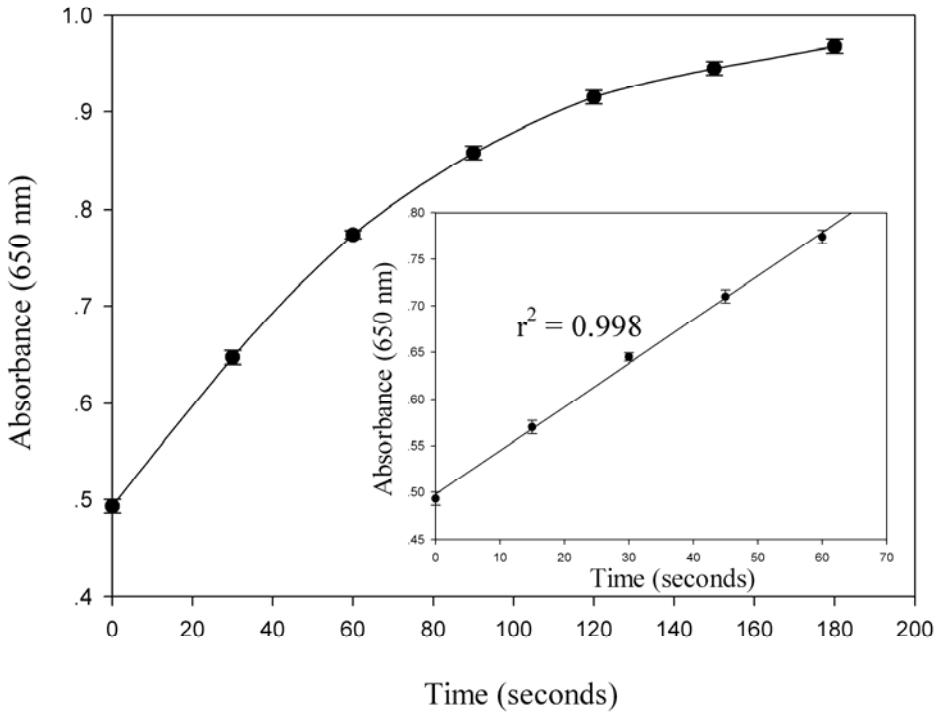

Figure 26. The plot of absorbance increments against calcium-arsenazo III reaction times by assaying the calcium concentration of 3 mg dL^{-1}.

2.4 pH of the carrier buffer

In this research, an alkaline pH region was selected for measuring calcium levels because the arsenazo III method sensitivity increased when compared to the reaction occurring in an acidic region. Hence, boric acid/sodium hydroxide solutions were used to maintain the pH in the range of 8, 8.5, and 9. The optimal concentration

of arsenazo III was prepared with three different pHs of 25 mM boric acid buffer containing 5 mM 8HQS. Under the alkaline environment, the 8HQS binds to magnesium; thus, it competes with calcium to form a complex with arsenazo III [51].

As shown in Figure 27, the analytical signals of the three different pHs of boric acid buffer were compared. Although the calcium-arsenazo III complexes at pH 9 provided the highest response signals, they were disregarded due to their narrow linearity. The pH 8 buffer was instead selected for all subsequent experiments because it provided a wider linearity, and up to 3 mg dL^{-1} of calcium could be assayed.

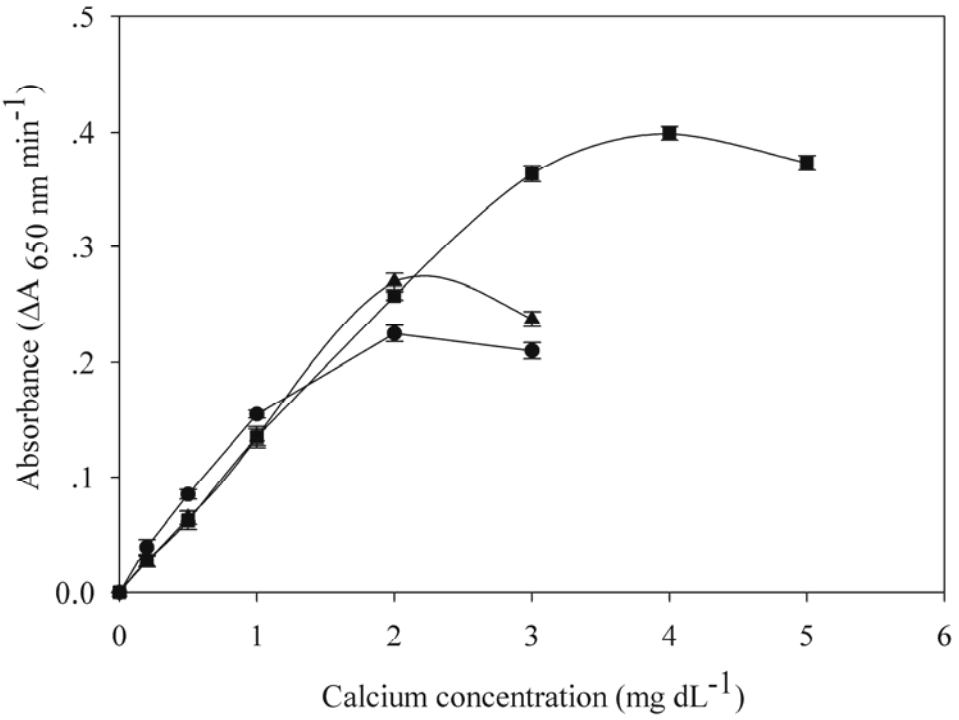

Figure 27. The effect of the carrier buffer pH to the assay signals (■) pH 8, (▲) pH 8.5, and (●) pH 9. Each concentration of calcium was assayed in duplicate and the standard deviation of assays was depicted as an error bar.

2.5 Concentration of arsenazo III

The effect of arsenazo III reagent concentration on the assay sensitivity was investigated in the range of 200-500 µM. Two levels of calcium standards were analysed (0.2 and 3 mg dL^{-1}). As shown in Figure 28, the results demonstrated that the sensitivity increased with an increasing arsenazo III concentration. However, when assaying with 3 mg dL^{-1} of calcium, concentrations above 400 µM did not improve the assay signal because a plateau response was likely obtained. This plateau implied that the saturation of arsenazo III dye with calcium took place at this concentration. It was also clearly observed that the background signals increased accordingly with the concentration of arsenazo III reagent. Hence, an arsenazo III concentration of 400 µM was selected as a compromise between sensitivity and acceptable background signal for all subsequent experiments.

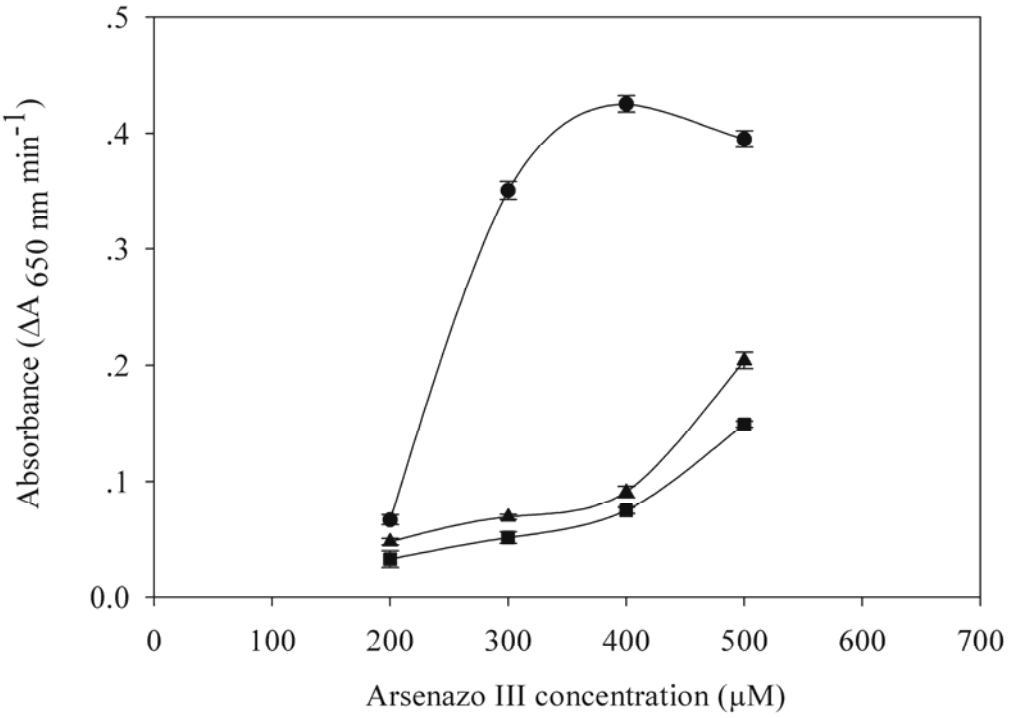

Figure 28. The effect of arsenazo III concentration on the response signals: (■) reagent blank, (▲) 0.2 mg dL^{-1} calcium, and (●) 3 mg dL^{-1} calcium.

2.6 Temperature

To maintain a constant temperature throughout the experiment, a temperature regulator optimised the temperature. To gauge the effect of temperature on the system, analytes were performed at 25, 30, 35, and 37°C. A calcium concentration of 3 mg dL^{-1} was assayed in duplicate at the four different temperatures. As shown in Figure 29, the temperature at 30°C was selected for further experiments because it provided the highest response signal. When the temperature was higher than 30°C, it could generate a large number of air bubbles. This effect of increasing air bubbles would interfere in the absorbance measurement affecting the assay reproducibility.

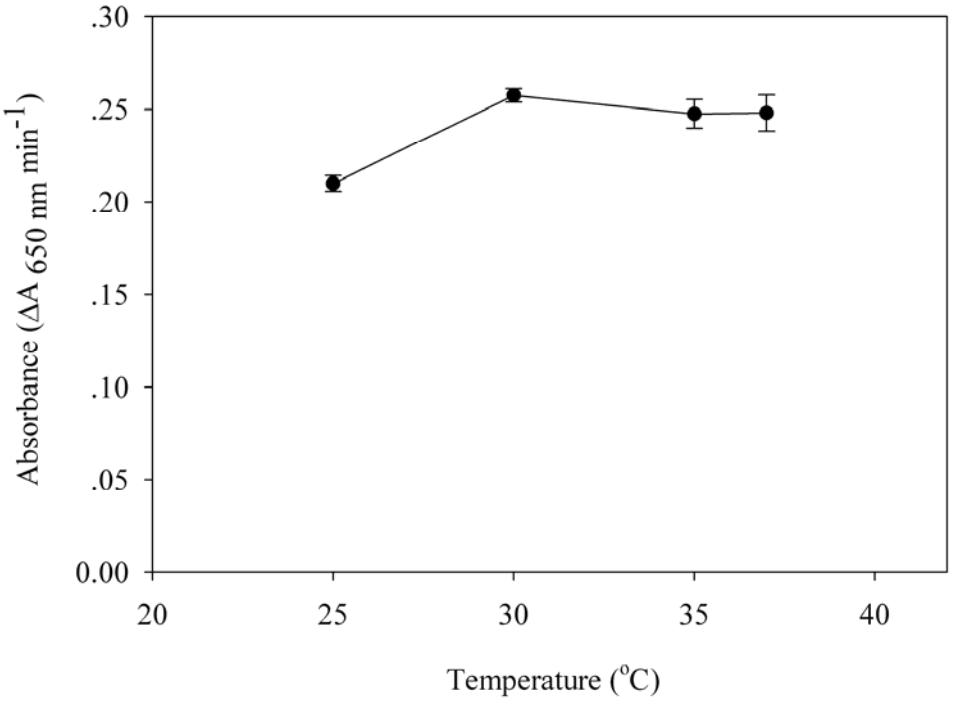

Figure 29. The effect of temperature on the absorbance signals for the measurement of calcium.

3. Assay characterisation

3.1 Linearity

Under the proper condition, the proportional relationship between the concentration of calcium and the analytical signal was plotted to produce an analytical curve. To construct an analytical curve for the calcium assay, the following conditions were utilised. The volumes of the sample and the Arsenazo III reagent were 2 and 25 μL, respectively. The assay was performed at 30°C, the reagent was composed of 400 μM arsenazo III in 25 mM boric acid, and pH was 8.0. The results are displayed in Figure 30, where the linear range was measured from 0.2 to 3 mg dL^{-1} of calcium (r^2 = 0.996), and the detection limit was found to be 0.138 mg dL^{-1} or 0.0345 mM (S/N=3), respectively.

Our proposed method is slightly more sensitive than the method described previously by Malcik et al. [22]; their detection limit is 0.085 mM. Additionally, the sensitivity of this system is similar to another method that used reflectance measurements of Arsenazo III immobilised polymer beads [26]; however, its detection limit was maximised at 0.0268 mM.

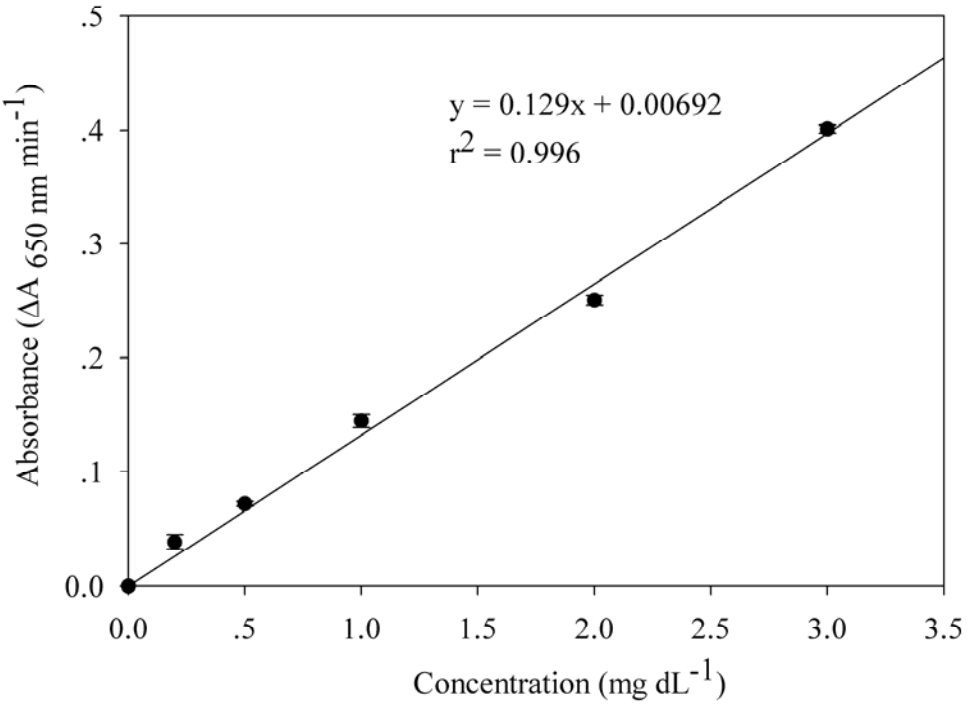

Figure 30. Analytical curve for the calcium assay based on an arsenazo III method using a microfluidic system.

3.2 Reproducibility and carry-over effect

Two levels of control serum were assayed for calcium content to study the reproducibility of the system. The results showed that within-run reproducibility was attained at 4.10% and 3.9% CVs, respectively, when performed with low- and high-level control serums on the same day (each concentrations n = 10). Moreover, run-to-run reproducibility was obtained at 4.6% CVs, as assessed on three different days (n =10). These results indicate that our proposed system provided good reproducibility.

Owing to the reusability of our microfluidic device, a carry-over effect should be considered. The carry-over effect study was performed following a method described in a previous study [128]. As shown in Table 10, the carry-over effect was calculated to be 1.98%, which is acceptable for the current system. Because the PDMS surface was regenerated using 1 M HCl after each assay, the carry-over effect was low to negligible. In addition, using an acid-washing step helped eliminate contaminated traces of calcium from the system before starting a new run.

Table 10. Percentage value of carry-over effect

Symbol	Calcium concentration (mg dL^{-1})	Absorbance (ΔA 650 nm min^{-1})	ΔAbsorbance ($\Delta A_{calcium}$-ΔA_{blank})	Percentage of Carry-over effect
Reagent blank	0	0.063		%Carry over = (b1-b3)/(a2-b3)
a1	3	0.392	0.329	1.98%
a2	3	0.395	0.332	
b1	0.2	0.197	0.134	
b2	0.2	0.199	0.136	
b3	0.2	0.193	0.13	

3.3 Interferences

In previous reports [11-12, 22], various substances that affect assay performance for calcium studies were investigated, including monovalent and divalent cations, trace metals, glucose, ascorbic acid, haemoglobin, and bilirubin. As haemolysis is a frequent chromophoric interference, our assay was investigated carefully by spiking with two different haemoglobin concentrations. Arsenazo III is also known to bind with other cations and form complexes. In particular, magnesium reacts with Arsenazo III at an alkaline pH. Magnesium is a divalent cation and is generally found in blood. However, due to the pH limitation, hydroxyquinoline-5-sulphonic acid (8HQS) was needed as a masking agent [52]. Besides magnesium, the other major cation in blood, such as sodium, was also examined in parallel.

A known amount of interference was spiked into the control serum samples, and then the percentage recovery was calculated from the ratio of the initial response signals to the spiked signals. As shown in Table 11, the results revealed that the interference from magnesium, iron, glucose, ascorbic acid, and sodium chloride were acceptable with the recoveries between 95.3%-103.7%. Comparatively, a haemoglobin concentration of 500 mg dL^{-1} affected the calcium assay with a recovery of 83.9%. However, when the concentration of haemoglobin decreased to 50 mg dL^{-1}, the percent of recovery became more acceptable at 100.7%. Considering bilirubin, the results displayed that 20 mg dL^{-1} could seriously interfere in the proposed assay. By contrast, 0.5 mg dL^{-1} of bilirubin was quite satisfactory, giving a recovery signal of 97.3%. Nevertheless, because bilirubin is usually low in human blood, this interference could be feasibly disregarded [34].

Table 11. Interferences effects on the measurement of calcium using the arsenazo III method.

Added interferences	Added concentration (mg dL^{-1})	%Recovery
Magnesium	123	95.3
Haemoglobin	500	83.9
	50	100.7
Bilirubin	20	81.2
	0.5	97.3
Iron	0.1	99.3
Glucose	10	103.7
Ascorbic acid	0.5	95.7
NaCl	900	96.3

3.4 Assay comparison

The assay comparison studies were performed with a conventional spectrometer method as a reference. Fifteen samples were tested for calcium content utilising our system in parallel with the current large-scale methods. Owing to the linearity of our system, ranging from 0.2 to 3 mg dL^{-1}, of calcium, the samples were diluted with saline before analysis. To get various amounts of analysts, including those with lower and higher than normal calcium levels, the real serum samples were spiked with low or high levels of calcium from the commercial control serums before assaying.

As shown in Figure 31, the regression equation was $y = 0.945x + 0.1064$ and $r^2 = 0.985$, which implies both methods are correlated. In addition, the results were further analysed with a Bland-Altman bias plot and a Passing-Bablok regression. Figure 32 (top) displays a scatter diagram of the differences plotted against the average values of the two methods. Both the upper and lower horizontal lines had a 95% confidence interval for their limit of agreement. Furthermore, the results demonstrated a good relationship between the proposed microfluidic system and the conventional spectrometer method because they both had a mean SD ± 1.96. In Figure 32 (bottom), the regression equation according to Passing and Bablok was $y = 0.9651x + 0.01756$. According to the 95% confidence interval noted above, the plotted graph's values for the y-intercept (0.01756) and the slope (0.9651) must be significantly reliable and fell in the range of -0.4207 to 0.06618 and 0.8874 to 1.0165, respectively. In other words, these data suggest that the proposed microfluidic system is highly correlated with the conventional spectrometer method, using an assay kit from Randox.

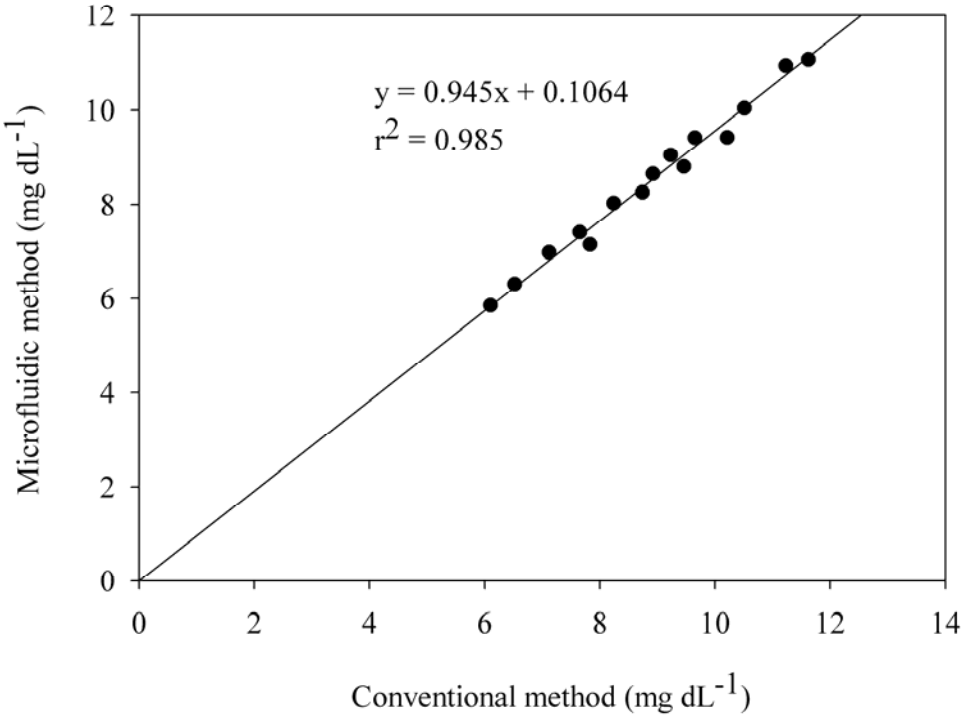

Figure 31. Correlation between the calcium assay as determined by the conventional method (X) and the proposed microfluidic system (Y). The regression equation was y = 0.945x + 0.1064 and r^2 = 0.985.

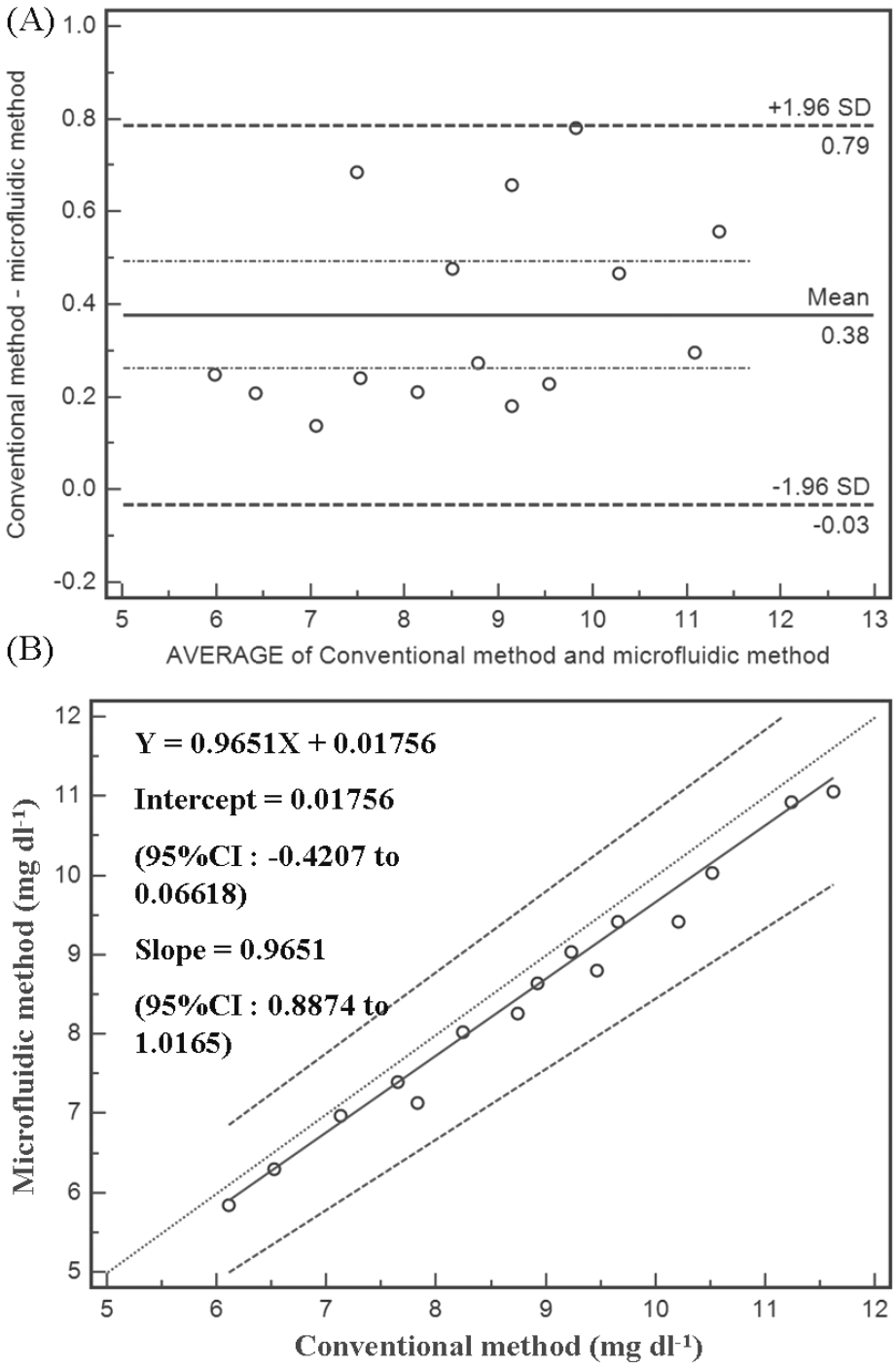

Figure 32. A detailed comparison of two different approaches for calcium assays: the proposed microfluidic system and a conventional method using (A) a Bland-Altman bias plot and (B) a Passing-Bablok regression analysis [127].

CHAPTER V

DISCUSSION AND CONCLUSION

1. Discussion

1.1 Fabrication and characterisation

In the previous study, Lin et al. [129] asserted that their microfluidic mixer could enhance the mixing performance when applying the liquids of high viscosity to their proposed design. Using this approach, the viscosity of blood, which is higher than that of water, is suitable for on-chip analysis. For this reason, the T-channel with a modified J-shaped structure was employed for our mixing purpose. The standard soft-lithography and replica molding procedure were used to produce the PDMS-glass layering of microfluidic devices. The fluorescence experimental verification was selected for evaluating the mixing efficiency due to its accuracy and efficiency. When the two different fluids (fluorescein solution and water) were dispersed to contact each other, there was no occurrence of chemical reaction. Hence, the mixing depends largely on the channel geometry. Compared to another technique, i.e. the reaction between the acids and bases, this method was used to quantify mixing by the change in pH values. The pH change relies on the reaction rates, which can cause an inaccurate measurement of mixing.

Based on the proposed design of T-type micromixer with four sets of ten J-shaped baffles in the main channel, the experimental results were in good agreement with the simulation results. The results indicated that the proposed micromixer would be effective for enhancing the mixing performance of the system. Although the mixing results from computational simulation and the captured fluorescence images

were verified to be similar, the percentage of mixing with the real fluorescence experiment was lower than that of the simulation results. The discrepancy between the experimental and simulated results was possibly the error in fabrication process. Therefore, both of experimental and stimulated models were not identical in character.

In order to study the effect of flow rate on mixing performance, the flow rate varied from 5 to 100 μL min^{-1}. As the flow rate increased from the flow rate of 5 to 20 μL min^{-1}, the mixing performance of our proposed design gradually decreased. While the flow rate continued to increase over 20 μL min^{-1}, it could sustain almost 90% mixing efficiency over the wide range of flow rates. The results could be implied that the mixing mechanism depends heavily on the diffusion at the low flow rate. At the higher flow rates, the mixing mechanism is based on the convection. When the flow rate was higher than 40 μL min^{-1}, the microfluidic devices always faced the problem with the leakage of device. Hence, the flow rate of 40 μL min^{-1} was selected as a compromise between mixing efficiency and pressure driven-force for all subsequent experiments.

1.2 Application for calcium assay

Recently, there have been several reports describing the microfluidic-based biochemical analysis systems. For example, Kim et al. [88] proposed an easily integrative and efficient micromixer and its application to the spectroscopic detection of glucose-catalyst reactions. In their work, the mixing of confluent liquid streams was achieved by “strong stretching and folding” which employed a three-dimensional microchannel structure. A novel in-plane passive microfluidic mixer with modified

Tesla structures was first put forward by Hong et al. [89]. They demonstrated that the mixing performance of the mixer was evaluated by comparing the measured pH values due to the installed pH sensors at the channel outlet. Based on the optical fibre sensor, Wu et al. [85] proposed the development of PDMS-based microfluidic device with integrated optical fibres for online monitoring of lactase.

As mentioned above, many researchers turned their attention to the incorporation of micromixer into biochemical microfluidic device. Many micromixer designs have been reported in the literature [85, 88-89, 129]. A three-dimensional microchannel structure for spectroscopic detection of glucose-catalyst reactions is a case in point [88]. Its appearance resembled an alligator's teeth, which provided an efficient mixing performance of two confluent liquid streams. Although it was a highly effective approach for the fluid mixing, it was complex in fabrication due to its 3D structure. Other example of microfluidic-based biochemical analysis was the study of on-line monitoring of lactase [85]. This system proved to be able to detect lactate, reasonable fast response time (about 130 s) and low detection limit. Nevertheless, the total length of main microchannel was very long.

With our proposed system, the absorbance detection of serum calcium assay could perform on-chip as a single-step microfluidic device. Sufficiently rapid, homogeneous mixing of the assay reagent and sample was achieved within the microchannels because of the planar micromixers with J-shaped obstacles. Obviously, this strategy was potentially accelerated by the uniform mixing of both reagents in the short mixing path of the microfluidic chip. The good reproducibility and satisfactory results of calcium determination were obtained from the integration of T-type microchannel with four sets of ten J-shaped baffles. Under the optimised condition, the

linear range was achieved from 0.2 to 3 mg dL^{-1} of calcium (r^2 = 0.996), with the detection limit of 0.138 mg dL^{-1} (S/N=3). In comparison to other works, our proposed method showed a more sensitivity to the method described by Malcik et al. [22].

Unless otherwise stated, the custom-made flow cell with a 1-cm path length incorporated into microchip could overcome the limitation of short optical path-length in microchannels. The two optical fibers were horizontally aligned to the flow cell and used to collect the data on absorption measurement. Using this configuration, we successfully improved the assay sensitivity of serum calcium for on-chip absorbance detection.

By comparison with other recent microfluidic systems, our proposed system was not only fully portable, but also corresponded closely to the concept of green chemistry. A remarkable decrease in reagent consumption and waste products was achieved when using this system. In addition, the proposed system offered the great potential for achieving a simplicity of fabrication and a reusable system. Owing to the reusability of our microfluidic device, a carry-over effect was under the consideration. According to a method described in a previous study [128], the study of carry-over effect was performed by analysing a high calcium concentration (3 mg dL^{-1}) in duplicate and following in triplicate with a low calcium concentration (0.2 mg dL^{-1}). The carry-over effect was calculated to be 1.98%, which was low and acceptable for the current system.

Apart from this, the developed method was found to have high specificity, i.e. not affected by other substances including magnesium, sodium, glucose, ascorbic acid, haemoglobin (50 mg dL^{-1}) and bilirubin (0.5 mg dL^{-1}) commonly found in blood. In comparison to a conventional spectrophotometric method, this portable,

microfluidic method correlated highly when evaluating serum samples (r^2 = 0.985*;* n= 15). The results implied that our proposed system could be used for determining the amount of calcium in serum samples. In other words, the proposed microfludic system has become the method of choice for serum calcium assay. This method is easy to perform and offers an accurate interpretation at clinically significant levels.

2. Conclusion

The main aim of this work is to develop the microfluidic system for serum calcium assays. Hence, the microfluidic simulation and experimental fluorescence set-up were carried out for characterising mixing performance. Apart from this, the applicability of the proposed microfluidic system was configured for assaying serum calcium based on the arsenazo III method. The study with its achievements is summarised below:

1. Characteristics of the proposed passive microfluidic mixer are as follow:
    1.1 According to the simulation results, the plain T-type micromixer was achieved the mixing percentage of ~ 60% homogeneity, whereas the T-type micromixer with four sets of ten J-shaped baffles in the main channel was achieved ~ 90% after passing all mixing regions.
    1.2 According to the captured fluorescence images, the plain T-type micromixer was achieved the mixing percentage of ~ 50% homogeneity, whereas the T-type micromixer with four sets of ten J-shaped baffles in the main channel was achieved ~ 85% after passing all mixing regions.
    1.3 Good agreement between simulation and fluorescence experimental results was obtained.

1.4 The homogeneous mixing was attained in a short time and within a limited length, which accounted for a 25-mm length.

2. Characteristics of the microfluidic system for calcium assay are as follows:

2.1 Under the proper condition, all the experiments were performed at 30 °C, the carrier buffer used was 25 mM boric acid (pH 8.0), at a constant flow rate of 40 μL min^{-1}.

2.2 Optimum ratio of sample-to-reagent was 2:25 μL. The injection valves was utilised to subject the 2-μL serum samples to the system, while a separate valve was used to load the 25-μL arsenazo III reagent (400 μM).

2.3 Reasonable fast response time was approximately within 60 seconds.

2.4 Excellent linear relationship (r^2 = 0.996) between the absorbance signal response and calcium concentration over a range of 0.2-3 mg dL^{-1} was obtained.

2.5 Good reproducibility based on low and high calcium tests with control serums, the within-run coefficient of variation (CVs) (4.10% and 3.91%: each concentrations n= 10), and the run-to-run CV (4.6%) were obtained (n= 30).

2.6 The carry-over effect of the method was 1.98%, which is acceptable for the current system.

2.7 The interference from magnesium, iron, sodium chloride, glucose, haemoglobin (50 mg dL^{-1}), bilirubin (0.5 mg dL^{-1}**)** and ascorbic acid were acceptable with the recoveries between 95.3%-103.7%.

2.8 Good agreement between the conventional spectrometer method and the proposed microfluidic method was observed (r^2 = 0.985) for analysis of calcium in serum samples. (n= 15)

With this proposed microfluidic system, the absorbance detection of calcium assays can be performed directly on-chip, while also being fully portable. From this point of view, this method proves promising to perform in field analyses of calcium from human samples or even from environmental samples. Additionally, this miniaturised system corresponds closely with the concept of green chemistry, which focuses on the reduction or elimination of toxic waste products.

REFERENCES

[1.] Polancic, J. E. Electrolytes. In M. L. Bishop, E. P. Fody, and L. E. Schoeff (ed.), Clinical Chemistry: Principles, Procedures, Correlations, pp. 314-342. Philadelphia: Lippincott Williams & Wilkins, 2005.

[2.] Carmeliet, G., Cromphaut, S. V., Daci, E., Maes, C., and Bouillon, R. Disorders of calcium homeostasis. Best Practice & Research Clinical Endocrinology & Metabolism. 17 (2003): 529-546.

[3.] Knecht, T. P., and Knecht, L. E. Parathyroid Function and Control for calcium Homeostasis. In M. L. Bishop, E. P. Fody, and L. E. Schoeff (ed.), Clinical Chemistry: Principles, Procedures, Correlations, pp. 457-474. Philadelphia: Lippincott Williams & Wilkins, 2005.

[4.] Smith Jr, J. C., Butrimovitz, G. P., and Purdy, W. C. Direct measurement of zinc in plasma by atomic absorption spectroscopy. Clinical Chemistry. 25 (1979): 1487.

[5.] Trudeau, D. L., and Freier, E. F. Determination of calcium in urine and serum by atomic absorption spectrophotometry (AAS). Clinical Chemistry. 13 (1967): 101.

[6.] Marshall, W. J., and Bangert, S. K. Clinical Chemistry. 5th Edition. St. Louis: Mosby, 2004.

[7.] Themelis, D. G., Tzanavaras, P. D., Anthemidis, A. N., and Stratis, J. A. Direct, selective flow injection spectrophotometric determination of calcium in wines using methylthymol blue and an on-line cascade dilution system. Analytica Chimica Acta. 402 (1999): 259-266.

[8.] Cowley, D. M., Mottram, B. M., Haling, N. B., and Sinton, T. J. Improved linearity of the calcium-cresolphthalein complexone reaction with sodium acetate. Clinical Chemistry. 32 (1986): 894.

[9.] Cohen, S. A., and Sideman, L. Modification of the o-cresolphthalein complexone method for determining calcium. Clinical Chemistry. 25 (1979): 1519.

[10.] Michaylova, V., and Ilkova, P. Photometric determination of micro amounts of calcium with arsenazo III. Analytica Chimica Acta. 53 (1971): 194-198.

[11.] Leary, N. O., Pembroke, A., and Duggan, P. F. Single stable reagent (Arsenazo III) for optically robust measurement of calcium in serum and plasma. Clinical Chemistry. 38 (1992): 904.

[12.] Morgan, B. R., Artiss, J. D., and Zak, B. Calcium determination in serum with stable alkaline Arsenazo III and triglyceride clearing. Clinical Chemistry. 39 (1993): 1608-1612.

[13.] Gindler, E. M., inventor; Pierce Chemical Company, assignee. Colorimetric determination of calcium in biological fluids. patent number 3,754,865. (1973)

[14.] Stavropoulos, W. S., Thiegs, B. J., and Mack, R. F., inventors; The Dow Chemical Company, assignee. Determination of calcium. patent number 3,938,954. (1976)

[15.] Armenta, S., Garrigues, S., and De la Guardia, M. Green analytical chemistry. TrAC Trends in Analytical Chemistry. 27 (2008): 497-511.

[16.] Whitesides, G. M. The origins and the future of microfluidics. Nature. 442 (2006): 368-373.

[17.] Sia, S. K., and Whitesides, G. M. Microfluidic devices fabricated in poly (dimethylsiloxane) for biological studies. Electrophoresis. 24 (2003): 3563-3576.

[18.] McDonald, J. C., and Whitesides, G. M. Poly (dimethylsiloxane) as a material for fabricating microfluidic devices. Accounts of Chemical Research. 35 (2002): 491-499.

[19.] Duffy, D. C., McDonald, J. C., Schueller, O. J. A., and Whitesides, G. M. Rapid prototyping of microfluidic systems in poly (dimethylsiloxane). Analytical Chemistry. 70 (1998): 4974-4984.

[20.] Minas, G., Wolffenbuttel, R. F., and Correia, J. H. An array of highly selective Fabry–Perot optical channels for biological fluid analysis by optical absorption using a white light source for illumination. Journal of Optics A: Pure and Applied Optics. 8 (2006): 272.

[21.] Minas, G., Wolffenbuttel, R. F., and Correia, J. H. A lab-on-a-chip for spectrophotometric analysis of biological fluids. Lab on a Chip. 5 (2005): 1303–1309.

[22.] Malcik, N., Ferrance, J. P., Landers, J. P., and Caglar, P. The performance of a microchip-based fiber optic detection technique for the determination of Ca2+ ions in urine. Sensors and Actuators B: Chemical. 107 (2005): 24-31.

[23.] Viskari, P. J., and Landers, J. P. Unconventional detection methods for microfluidic devices. Electrophoresis. 27 (2006): 1797-1810.

[24.] Laiwattanapaisal, W., Songjaroen, T., Maturos, T., Lomas, T., Sappat, A., and Tuantranont, A. On-Chip Immunoassay for Determination of Urinary Albumin. Sensors. 9 (2009): 10066-10079.

[25.] Songjaroen, T., Maturos, T., Sappat, A., Tuantranont, A., and Laiwattanapaisal, W. Portable microfluidic system for determination of urinary creatinine. Analytica Chimica Acta. 647 (2009): 78-83.

[26.] Caglar, P., Tuncel, S. A., Malcik, N., Landers, J. P., and Ferrance, J. P. A microchip sensor for calcium determination. Analytical and Bioanalytical Chemistry. 386 (2006): 1303-1312.

[27.] Nguyen, T. N. T., Kim, M. C., Park, J. S., and Lee, N. E. An effective passive microfluidic mixer utilizing chaotic advection. Sensors & Actuators: B Chemical. 132 (2008): 172-181.

[28.] Ismagilov, R. F., Rosmarin, D., Kenis, P. J. A., Chiu, D. T., Zhang, W., Stone, H. A., et al. Pressure-driven laminar flow in tangential microchannels: an elastomeric microfluidic switch. Analytical Chemistry. 73 (2001): 4682-4687.

[29.] Kenis, P. J. A., Ismagilov, R. F., Takayama, S., Whitesides, G. M., Li, S., and White, H. S. Fabrication inside microchannels using fluid flow. Accounts of Chemical Research. 33 (2000): 841-847.

[30.] Nguyen, N. T., and Wu, Z. Micromixers—a review. Journal of Micromechanics and Microengineering. 15 (2005): R1.

[31.] Hessel, V., Löwe, H., and Schönfeld, F. Micromixers--a review on passive and active mixing principles. Chemical Engineering Science. 60 (2005): 2479-2501.

[32.] Bhagat, A. A. S., and Papautsky, I. Enhancing particle dispersion in a passive planar micromixer using rectangular obstacles. Journal of Micromechanics and Microengineering. 18 (2008): 085005.

[33.] Bhagat, A. A. S., Peterson, E. T. K., and Papautsky, I. A passive planar micromixer with obstructions for mixing at low Reynolds numbers. Journal of Micromechanics and Microengineering. 17 (2007): 1017.

[34.] Roberts, W. L., McMillin, G. A., Burtis, C. A., and Bruns, D. E. Reference information for the clinical laboratory. In C. A. Burtis, E. R. Ashwood, and D. E. Bruns (ed.), TIETZ Fundamentals of Clinical Chemistry, pp. 836-873. St. Louis: Saunders Elsevier, 2008.

[35.] Endres, D. B., and Rude, R. K. Disorders of bone. In C. A. Burtis, E. R. Ashwood, and D. E. Bruns (ed.), TIETZ Fundamentals of Clinical Chemistry, pp. 711-734. St. Louis Saunders: Elsevier, 2008.

[36.] Rasmussen, H., DeLuca, H., Arnaud, C., Hawker, C., and Vonstedingk, M. The relationship between vitamin D and parathyroid hormone. The Journal of Clinical Investigation. 42 (1963): 1940.

[37.] Glajchen, N., Thomas, S., Jowell, P., Epstein, S., Ismail, F., and Fallon, M. The effect of high-dose salmon calcitonin on bone mineral metabolism in the normal rat. Calcified Tissue International. 46 (1990): 28-32.

[38.] Ljunghall, S., Gärdsell, P., Johnell, O., Larsson, K., Lindh, E., Obrant, K., et al. Synthetic human calcitonin in postmenopausal osteoporosis: a placebo-controlled, double-blind study. Calcified Tissue International. 49 (1991): 17-19.

[39.] Zilva, J. F., Pannall, P. R., and Mayne, P. D. Clinical Chemistry in Diagnosis and Treatment. 5th Edition. Sevenoaks: ELBS with Edward Arnold, 1998.

[40.] Shu, F. R., Mu, X., Chung, S. C., Houben, P. J., and Kessler, J. T., inventors; Beckman Instruments Inc., assignee. Diluent and method for determination of total calcium. patent number 5,424,214. (1995)

[41.] Nonobe, M., Nishida, H., and Fujita, T., inventors; Oriental Yeast Co., Ltd., assignee. Method of determination of calcium. patent number 5,618,684. (1997)

[42.] Mihara, T., Kondo, H., and Nagata, K., inventors; Unitika Ltd., assignee. Reagent for calcium ion level determination. patent number 5,902,730. (1999)

[43.] Tadano, T., Miike, A., Kayahara, N., and Umemoto, J., inventors; Kyowa Medex Co., Ltd., assignee. Method for measurement of ionized calcium. patent number 5,840,512. (1998)

[44.] Sugano, M., Yamauchi, K., Sugano, K., Kawasaki, K., Tozuka, M., Katsuyama, T., et al. New enzymatic assay using phospholipase D to measure total calcium in serum. Clinical Chemistry. 51 (2005): 1021.

[45.] Hinson, J. A., and Neal, R. A. An examination of the oxidation of aldehydes by horse liver alcohol dehydrogenase. Journal of Biological Chemistry. 247 (1972): 7106.

[46.] Goriushkina, T., Shkotova, L., Gayda, G., Klepach, H., Gonchar, M., Soldatkin, A., et al. Amperometric biosensor based on glycerol oxidase for glycerol determination. Sensors and Actuators B: Chemical. 144 (2010): 361-367.

[47.] Narrod, S., and Jakoby, W. Metabolism of ethanolamine. An ethanolamine oxidase. The Journal of Biological Chemistry. 239 (1964): 2189.

[48.] Chowdhury, E. K., Higuchi, K., Nagata, S., and Misono, H. A novel NADP (+)-dependent serine dehydrogenase from Agrobacterium tumefaciens. Bioscience, Biotechnology, and Biochemistry. 61 (1997): 152.

[49.] Moorehead, W. R., and Biggs, H. G. 2-Amino-2-methyl-1-propanol as the alkalizing agent in an improved continuous-flow cresolphthalein complexone procedure for calcium in serum. Clinical Chemistry. 20 (1974): 1458.

[50.] Stern, J., and Lewis, W. H. P. The colorimetric estimation of Calcium in serum with O-cresolphthalein Complexone. Clinica Chimica Acta. 2 (1957): 576-580.

[51.] Denney, J. W., inventor; Synermed, Inc., assignee. Reagent and methods for calcium determination. patent number 5,057,435. (1991)

[52.] Artiss, J. D., Morgan, B. R., and Zak, B., inventors; The board of Governors of Wayne State University, assignee. Method and compositions for the determination of serum calcium using asenazo III. patent number 5,215,922. (1993)

[53.] Corns, C. M. A new colorimetric method for the measurement of serum calcium using a zinc-zincon indicator. Annals of Clinical Biochemistry. 24 (1987): 591.

[54.] Bauer, P. J. Affinity and stoichiometry of calcium binding by arsenazo III. Analytical Biochemistry. 110 (1981): 61-72.

[55.] Pybus, J., Feldman, F., and Bowers Jr, G. Measurement of total calcium in serum by atomic absorption spectrophotometry, with use of a strontium internal reference. Clinical Chemistry. 16 (1970): 998.

[56.] Helger, R., inventor; Merck Patent Gesellschuft mit beschrankter Haftung, assignee. Agent and method for determination of calcium. patent number 3,798,000. (1974)

[57.] Rathje, W., inventor; Boehringer Mannheim GMBH, assignee. Reagent for the determination of calcium. patent number 3,854,880. (1974)

[58.] Noda, K., Kojima, R., and Katayama, K., inventors; Nitto Boseki CO., LTD., assignee. Regent for determination of calcium and determination method. patent number US2006/0008915 A1. (2006)

[59.] He, H., and Lin, C., inventors; OPTI Medical Systems, Inc., assignee. Chromoionophore and method of determining calcium ions. patent number US2007/0259438 A1. (2007)

[60.] Gravesen, P., Branebjerg, J., and Jensen, O. S. Microfluidics-a review. Journal of Micromechanics and Microengineering. 3 (1993): 168.

[61.] El Moctar, A. O., Aubry, N., and Batton, J. Electro-hydrodynamic micro-fluidic mixer. Lab on a Chip. 3 (2003): 273-280.

[62.] Oddy, M. H., Santiago, J. G., and Mikkelsen, J. C. Electrokinetic instability micromixing. Analytical Chemistry. 73 (2001): 5822-5832.

[63.] Yang, Z., Matsumoto, S., Goto, H., Matsumoto, M., and Maeda, R. Ultrasonic micromixer for microfluidic systems. Sensors and Actuators A: Physical. 93 (2001): 266-272.

[64.] Bau, H. H., Zhong, J., and Yi, M. A minute magneto hydro dynamic (MHD) mixer. Sensors & Actuators: B Chemical. 79 (2001): 207-215.

[65.] Tsai, J. H., and Lin, L. Active microfluidic mixer and gas bubble filter driven by thermal bubble micropump. Sensors & Actuators: A Physical. 97 (2002): 665-671.

[66.] Munson, M. S., and Yager, P. Simple quantitative optical method for monitoring the extent of mixing applied to a novel microfluidic mixer. Analytica Chimica Acta. 507 (2004): 63-71.

[67.] Schwesinger, N., Frank, T., and Wurmus, H. A modular microfluid system with an integrated micromixer. Journal of Micromechanics and Microengineering. 6 (1996): 99.

[68.] Soleymani, A., Kolehmainen, E., and Turunen, I. Numerical and experimental investigations of liquid mixing in T-type micromixers. Chemical Engineering Journal. 135 (2008): S219-S228.

[69.] Gobby, D., Angeli, P., and Gavriilidis, A. Mixing characteristics of T-type microfluidic mixers. Journal of Micromechanics and Microengineering. 11 (2001): 126.

[70.] Hardt, S., and Schönfeld, F. Laminar mixing in different interdigital micromixers: II. Numerical simulations. AIChE Journal. 49 (2003): 578-584.

[71.] Hessel, V., Hardt, S., Löwe, H., and Schönfeld, F. Laminar mixing in different interdigital micromixers: I. Experimental characterization. AIChE Journal. 49 (2003): 566-577.

[72.] Voldman, J., Gray, M. L., and Schmidt, M. A. An integrated liquid mixer/valve. Journal of Microelectromechanical Systems. 9 (2000): 295-302.

[73.] Kim, D. S., Lee, S. W., Kwon, T. H., and Lee, S. S. A barrier embedded chaotic micromixer. Journal of Micromechanics and Microengineering. 14 (2004): 798-805.

[74.] Stroock, A. D., Dertinger, S. K. W., Ajdari, A., Mezic, I., Stone, H. A., and Whitesides, G. M. Chaotic mixer for microchannels. Science. 295 (2002): 647.

[75.] Xia, H. M., Wan, S. Y. M., Shu, C., and Chew, Y. T. Chaotic micromixers using two-layer crossing channels to exhibit fast mixing at low Reynolds numbers. Lab on a Chip. 5 (2005): 748-55.

[76.] Park, J. M., Seo, K. D., and Kwon, T. H. A chaotic micromixer using obstruction-pairs. Journal of Micromechanics and Microengineering. 20 (2010): 015023.

[77.] Paik, P., Pamula, V. K., and Fair, R. B. Rapid droplet mixers for digital microfluidic systems. Lab on a Chip. 3 (2003): 253-259.

[78.] Stone, Z. B., and Stone, H. A. Imaging and quantifying mixing in a model droplet micromixer. Physics of Fluids. 17 (2005): 063103.

[79.] Chung, C. K., and Shih, T. R. Effect of geometry on fluid mixing of the rhombic micromixers. Microfluidics and Nanofluidics. 4 (2008): 419-425.

[80.] Jen, C. P., Wu, C. Y., and Lin, Y. C. Design and simulation of the micromixer with chaotic advection in twisted microchannels. Lab on a Chip. 3 (2003): 77-81.

[81.] Mouza, A. A., Patsa, C. M., and Schönfeld, F. Mixing performance of a chaotic micro-mixer. Chemical Engineering Research and Design. 86 (2008): 1128-1134.

[82.] Tsui, Y. Y., Yang, C. S., and Hsieh, C. M. Evaluation of the Mixing Performance of the Micromixers With Grooved or Obstructed Channels. Journal of Fluids Engineering. 130 (2008): 071102.

[83.] Hossain, S., Ansari, M. A., and Kim, K. Y. Evaluation of the mixing performance of three passive micromixers. Chemical Engineering Journal. 150 (2009): 492-501.

[84.] Liu, R. H., Stremler, M. A., Sharp, K. V., Olsen, M. G., Santiago, J. G., Adrian, R. J., et al. Passive mixing in a three-dimensional serpentine microchannel. Journal of Microelectromechanical Systems. 9 (2000): 190-197.

[85.] Wu, M. H., Wang, J., Taha, T., Cui, Z., and Urban, J. P. G. Study of on-line monitoring of lactate based on optical fibre sensor and in-channel mixing mechanism. Biomedical Microdevices. 9 (2007): 167-174.

[86.] Jeon, W., and Shin, C. B. Design and simulation of passive mixing in microfluidic systems with geometric variations. Chemical Engineering Journal. 152 (2009): 575-582.

[87.] Kee, S. P., and Gavriilidis, A. Design and characterisation of the staggered herringbone mixer. Chemical Engineering Journal. 142 (2008): 109-121.

[88.] Kim, D. J., Oh, H. J., Park, T. H., Choo, J. B., and Lee, S. H. An easily integrative and efficient micromixer and its application to the spectroscopic detection of glucose-catalyst reactions. The Analyst. 130 (2005): 293-298.

[89.] Hong, C. C., Choi, J. W., and Ahn, C. H. A novel in-plane passive microfluidic mixer with modified Tesla structures. Lab on a Chip. 4 (2004): 109-113.

[90.] Unger, M. A., Chou, H. P., Thorsen, T., Scherer, A., and Quake, S. R. Monolithic microfabricated valves and pumps by multilayer soft lithography. Science. 288 (2000): 113.

[91.] Jansen, H., Gardeniers, H., Boer, M., Elwenspoek, M., and Fluitman, J. A survey on the reactive ion etching of silicon in microtechnology. Journal of Micromechanics and Microengineering. 6 (1996): 14.

[92.] Dolnik, V., Liu, S., and Jovanovich, S. Capillary electrophoresis on microchip. Electrophoresis. 21 (2000): 41-54.

[93.] McCormick, R. M., Nelson, R. J., Alonso-Amigo, M. G., Benvegnu, D. J., and Hooper, H. H. Microchannel electrophoretic separations of DNA in injection-molded plastic substrates. Analytical Chemistry. 69 (1997): 2626-2630.

[94.] Qin, D., Xia, Y., Rogers, J., Jackman, R., Zhao, X. M., and Whitesides, G. Microfabrication, microstructures and microsystems. Microsystem Technology in Chemistry and Life Science. (1998): 1-20.

[95.] Martynova, L., Locascio, L. E., Gaitan, M., Kramer, G. W., Christensen, R. G., and MacCrehan, W. A. Fabrication of plastic microfluid channels by imprinting methods. Analytical Chemistry. 69 (1997): 4783-4789.

[96.] Kane, R. S., Takayama, S., Ostuni, E., Ingber, D. E., and Whitesides, G. M. Patterning proteins and cells using soft lithography. Biomaterials. 20 (1999): 2363-2376.

[97.] Thorslund, S., Sanchez, J., Larsson, R., Nikolajeff, F., and Bergquist, J. Functionality and stability of heparin immobilized onto poly

(dimethylsiloxane). Colloids and Surfaces B: Biointerfaces. 45 (2005): 76-81.

[98.] Thorslund, S., Sanchez, J., Larsson, R., Nikolajeff, F., and Bergquist, J. Bioactive heparin immobilized onto microfluidic channels in poly (dimethylsiloxane) results in hydrophilic surface properties. Colloids and Surfaces B: Biointerfaces. 46 (2005): 240-247.

[99.] Thorslund, S., Lindberg, P., Andr n, P. E., Nikolajeff, F., and Bergquist, J. Electrokinetic driven microfluidic system in poly (dimethylsiloxane) for mass spectrometry detection integrating sample injection, capillary electrophoresis, and electrospray emitter on chip. Electrophoresis. 26 (2005): 4674-4683.

[100.] Thorslund, S., and Nikolajeff, F. Instant oxidation of closed microchannels. Journal of Micromechanics and Microengineering. 17 (2007): N16.

[101.] Majumdar, Z. K., Sutin, J. D. B., and Clegg, R. M. Microfabricated continuous-flow, turbulent, microsecond mixer. Review of Scientific Instruments. 76 (2005): 125103.

[102.] Sudarsan, A. P., and Ugaz, V. M. Fluid mixing in planar spiral microchannels. Lab on a Chip. 6 (2006): 74-82.

[103.] Jayaraj, S., Kang, S., and Suh, Y. K. A review on the analysis and experiment of fluid flow and mixing in micro-channels. Journal of Mechanical Science and Technology. 21 (2007): 536-548.

[104.] Wang, S., Jiao, Z., Huang, X., Yang, C., and Nguyen, N. Acoustically induced bubbles in a microfluidic channel for mixing enhancement. Microfluidics and Nanofluidics. 6 (2009): 847-852.

[105.] Wu, H. Y., and Liu, C. H. A novel electrokinetic micromixer. Sensors and Actuators A: Physical. 118 (2005): 107-115.

[106.] Tan, H. Y., Loke, W. K., Tan, Y. T., and Nguyen, N. T. A lab-on-a-chip for detection of nerve agent sarin in blood. Lab on a Chip. 8 (2008): 885-891.

[107.] Noda, T., Takao, H., Yoshioka, K., Oku, N., Ashiki, M., Sawada, K., et al. Performance of absorption photometry microchip for blood hemoglobin measurement integrated with processing circuits and Si (1 1 0) 45 mirrors. Sensors and Actuators B: Chemical. 119 (2006): 245-250.

[108.] Duggan, M. P., McCreedy, T., and Aylott, J. W. A non-invasive analysis method for on-chip spectrophotometric detection using liquid-core waveguiding within a 3D architecture. The Analyst. 128 (2003): 1336-1340.

[109.] Leelasattarathkul, T., Liawruangrath, S., Rayanakorn, M., Liawruangrath, B., Oungpipat, W., and Youngvises, N. Greener analytical method for the determination of copper (II) in wastewater by micro flow system with optical sensor. Talanta. 72 (2007): 126-131.

[110.] Chau, L. K., Osborn, T., Wu, C. C., and Yager, P. Microfabricated silicon flow-cell for optical monitoring of biological fluids. Analytical Sciences. 15 (1999): 721-724.

[111.] Nakanishi, H., Nishimoto, T., Kanai, M., Saitoh, T., Nakamura, R., Yoshida, T., et al. Condition optimization, reliability evaluation of SiO2-SiO2 HF bonding and its application for UV detection micro flow cell. Sensors and Actuators A: Physical. 83 (2000): 136-141.

[112.] Salimi-Moosavi, H., Jiang, Y., Lester, L., McKinnon, G., and Harrison, D. J. A multireflection cell for enhanced absorbance detection in microchip-based capillary electrophoresis devices. Electrophoresis. 21 (2000): 1291-1299.

[113.] Liang, Z., Chiem, N., Ocvirk, G., Tang, T., Fluri, K., and Harrison, D. J. Microfabrication of a planar absorbance and fluorescence cell for integrated capillary electrophoresis devices. Analytical Chemistry. 68 (1996): 1040-1046.

[114.] Kruanetr, S., Liawruangrath, S., and Youngvises, N. A simple and green analytical method for determination of iron based on micro flow analysis. Talanta. 73 (2007): 46-53.

[115.] Bargiel, S., Górecka-Drzazga, A., Dziuban, J. A., Prokaryn, P., Chudy, M., Dybko, A., et al. Nanoliter detectors for flow systems. Sensors and Actuators A: Physical. 115 (2004): 245-251.

[116.] Jindal, R., and Cramer, S. M. On-chip electrochromatography using sol-gel immobilized stationary phase with UV absorbance detection. Journal of Chromatography A. 1044 (2004): 277-285.

[117.] Thorslund, S., Klett, O., Nikolajeff, F., Markides, K., and Bergquist, J. A hybrid poly (dimethylsiloxane) microsystem for on-chip whole blood filtration optimized for steroid screening. Biomedical Microdevices. 8 (2006): 73-79.

[118.] Lien, K. Y., Liu, C. J., Kuo, P. L., and Lee, G. B. Microfluidic system for detection of -thalassemia-1 deletion using saliva samples. Analytical Chemistry. 81 (2009): 4502-4509.

[119.] Wolf, M., Juncker, D., Michel, B., Hunziker, P., and Delamarche, E. Simultaneous detection of C-reactive protein and other cardiac markers in human plasma using micromosaic immunoassays and self-regulating microfluidic networks. Biosensors and Bioelectronics. 19 (2004): 1193-1202.

[120.] Kurita, R., Yokota, Y., Sato, Y., Mizutani, F., and Niwa, O. On-chip enzyme immunoassay of a cardiac marker using a microfluidic device combined with a portable surface plasmon resonance system. Analytical Chemistry. 78 (2006): 5525-5531.

[121.] Sato, K., Tokeshi, M., Kimura, H., and Kitamori, T. Determination of carcinoembryonic antigen in human sera by integrated bead-bed immunoasay in a microchip for cancer diagnosis. Analytical Chemistry. 73 (2001): 1213-1218.

[122.] Maeng, J. H., Lee, B. C., Ko, Y. J., Cho, W., Ahn, Y., Cho, N. G., et al. A novel microfluidic biosensor based on an electrical detection system for alpha-fetoprotein. Biosensors and Bioelectronics. 23 (2008): 1319-1325.

[123.] Panini, N. V., Messina, G. A., Salinas, E., Fernández, H., and Raba, J. Integrated microfluidic systems with an immunosensor modified with carbon nanotubes for detection of prostate specific antigen (PSA) in human serum samples. Biosensors and Bioelectronics. 23 (2008): 1145-1151.

[124.] Sato, K., Tokeshi, M., Odake, T., Kimura, H., Ooi, T., Nakao, M., et al. Integration of an immunosorbent assay system: analysis of secretory human immunoglobulin A on polystyrene beads in a microchip. Analytical Chemistry. 72 (2000): 1144-1147.

[125.] Grabowska, I., Chudy, M., Dybko, A., and Brzozka, Z. Determination of creatinine in clinical samples based on flow-through microsystem. Analytica Chimica Acta. 540 (2005): 181-185.

[126.] Wiese, G., Barthel, S. R., and Dimitroff, C. J. Analysis of physiologic E-selection-mediated leukocyte rolling on microvascular. Journal of Visualized Experiments. (2009).

[127.] Boonyasit, Y., Maturos, T., Sappat, A., Jomphoak, A., Tuantranont, A., and Laiwattanapaisal, W. Passive micromixer integration with a microfluidic chip for calcium assay based on the arsenazo III method. BioChip Journal. 5 (2011): 1-7.

[128.] Haeckel, R. Proposals for the description and measurement of carry-over effects in clinical chemistry. Pure and Applied Chemistry. 63 (1991): 301-306.

[129.] Lin, Y. C., Chung, Y. C., and Wu, C. Y. Mixing enhancement of the passive microfluidic mixer with J-shaped baffles in the tee channel. Biomedical Microdevices. 9 (2007): 215-221.

Appendix

APPENDIX

Reagent preparation

1. Calcium stock standards (200 mg dL^{-1})

Calcium carbonate	2.5 g
1 M HCL	60 mL
Milli-Q water	500 mL

The calcium carbonate was baked before use. Working calcium standards were freshly prepared by diluting stock solution in boric acid buffer.

2. Stock of arsenazo III (1,000 µM)

Arsenazo III	77.6 mg
Milli-Q water	100 mL

3. Preparation of 8-Hydroxyquinoline-5-sulphonic acid (8HQS, 10 mM)

8HQS	2.3 mg
Boric acid buffer	500 µL

4. 50 mM Boric acid buffer

Boric acid	309.2 mg

The pH was adjusted to the desired pH with NaOH. The buffer was prepared in Milli-Q water and filtered by 0.45 µm cellulose acetate membrane.

VITAE

Yuwadee Boonyasit obtained her B.Sc. in Medical Technology from Chulalongkorn University in 2008, and enrolled in Clinical Biochemistry and Molecular Medicine Program (M.Sc.) in 2009. When she was undergraduate student, she received the Thailand Advanced Institute of Science and Technology's Pilot Project scholarship from the National Science and Technology Development Agency (NSTDA). Apart from this, she also received the Thailand Graduate Institute of Science and Technology scholarship (under the contract no. TG-44-09-51-094M), the CU Graduate School Thesis Grant, and the financial support for Master's students to present academic papers in a foreign country from the Graduate School.